THESIS FOR THE DEGREE OF DOCTOR OF PHILOSOPHY

Molecular Doping of Polar Conjugated Polymers

DAVID KIEFER

CHALMERS

Department of Chemistry and Chemical Engineering
CHALMERS UNIVERSITY OF TECHNOLOGY
Göteborg, Sweden 2019

Molecular Doping of Polar Conjugated Polymers
DAVID KIEFER
ISBN 978-91-7905-114-3

Doktorsavhandlingar vid Chalmers tekniska högskola
Ny serie nr. 4581
ISSN 0346-718X
Department of Chemistry and Chemical Engineering

Chalmers University of Technology
SE-412 96 Göteborg
Sweden
Telephone: +46 (0)31-772 1000

Cover:
Ball-and-stick model of an F4TCNQ molecule with two lightning bolts symbolizing double doping. (Design by Ella Maru studio)

Chalmers Reproservice
Göteborg, Sweden 2019

Molecular Doping of Polar Conjugated Polymers
DAVID KIEFER
Department of Chemistry and Chemical Engineering

Chalmers University of Technology

Abstract

Organic semiconductors may enable a wide range of flexible electronics, such as flexible displays or solar cells. Conjugated polymers constitute one of the most widely studied class of organic semiconductors. Molecular doping is an important tool to adjust their electrical conductivity through introduction of negative or positive charges by addition of molecular dopants. However, solution-processing of conjugated polymers with molecular dopants is limited due to precipitation and a low number of charges formed per dopant molecule as a result of dopant aggregation or inappropriate energy levels. Thus, large amounts of dopant are required that compromise the nanostructure of conjugated polymers and in turn reduce the electrical conductivity, which is furthermore sensitive to elevated temperatures or the exposure to air in case of n-doping. Therefore, ways that mitigate processing issues and increase the efficiency and stability of molecular doping are highly desired.

This thesis explores several concepts that may allow to improve the efficiency of molecular doping. A reduction of the required amount of dopant molecules is achieved by enhancing the compatibility of conjugated polymer:dopant pairs, which results in increased numbers of charges that are created per dopant molecule. In particular, polar side chains on conjugated polymers permit processing of polymer:dopant pairs from the same solution and largely suppress dopant aggregation resulting in improved electrical conductivity for p- and n-doping. Additionally, both the thermal stability of p-doped and air stability of n-doped films are found to benefit from polar side chains. Further, a low ionisation energy of conjugated polymers gives rise to dianion formation of common p-dopants. This double doping results in formation of two charges per dopant molecule and, thus, allows doubling of the doping efficiency. The concepts presented in this thesis provide several important design rules to guide the development of more efficient and stable molecularly doped conjugated polymers.

Keywords: molecular doping, polar conjugated polymer, compatibility, double doping, dopant dianion, thermal stability, air stability

Acknowledgements

After nearly five years of research at Chalmers – one as Master and four as PhD student – there are of course many people that I owe a great debt of gratitude:

First and foremost, I want to thank Christian Müller for guiding me over this whole time. I truly appreciated your open ear for any kind of problem and your open mindset to learn from each other.

I especially want to thank the people at Chalmers that worked very closely with me and that I have learned so much from. Renee, a special thanks for all our scientific discussions and for making all those polymers, which truly made my PhD a whole lot easier. Anna H. and Liyang, thanks for being awesome scientists and amazing colleagues. Thanks also to the (summer) interns I had the pleasure to work with and that were a great help with some of the experiments: Dominik, Alex C. and Anaïs.

I also want to thank those people outside of Chalmers that I had the privilege to collaborate with; in particular Alex Giovannitti from Imperial College for sending all those great materials and Hengda Sun and Simone Fabiano from Linköping University, Campus Norrköping, for hosting me several times.

Thanks to everyone on the '8th floor' for being great colleagues and creating an awesome work environment. Special thanks to Lotta for keeping us all going and for encouraging me to speak Swedish when I first started here. Tack! Thanks to all the awesome past and current people in the 'Müller group' that I didn't mention yet: Mattias, Amaia, Jason, Massi, Jonna, Anja, Anna P., Ida, Yingwei, Sepideh, Sandra, Sozan, Desalegn, Amir. Thanks to my office mates over the years: First, the group of Master students in the 'Master room'; then, Jonna and Alicja; and finally, the Annas and Jiamin. It was a pleasure to share an office with you guys.

Mattias and Johnas, thanks for being great friends and the occasional Friday lunch beer and afterwork. Skåll!

Ewa, thank you for keeping up with my moods and being by my side. Kocham cię!

Last, but not least, I want to thank my family: Elke, Peter und Nora, ohne euch wäre ich nicht wo ich heute bin. Danke für all Eure Liebe und Unterstützung.

David

Nomenclature

4T	quaterthiophene
α	Seebeck coefficient
BBL	poly(benzimidazobenzophenanthroline)
BCF	tris(pentafluorophenyl)borane
CV	cyclic voltammetry
DDQ	2,3-dichloro-5,6-dicyano-p-benzoquinone
DFT	density functional theory
DPP	diketopyrrolopyrrole
ε	relative dielectric constant
ε_0	vacuum dielectric constant
EA	electron affinity
E_g	band gap
EPR	electron paramagnetic resonance
ε_r	absolute dielectric constant
F2TCNQ	2,5-difluoro-7,7,8,8-tetracyanoquinodimethane
F4TCNQ	2,3,5,6-tetrafluoro-7,7,8,8-tetracyanoquinodimethane
F6TCNNQ	1,3,4,5,7,8-hexafluoro-tetracyanonaphthoquinodimethane
FTIR	Fourier-transform infrared spectroscopy
FTS	(tridecafluoro-1,1,2,2-tetrahydrooctyl)trichlorosilane
GIWAXS	grazing-incidence wide-angle X-ray scattering
HOMO	highest occupied molecular orbital
IE	ionisation energy
$\varkappa$	thermal conductivity
k_e	Coulomb constant
LUMO	lowest unoccupied molecular orbital
μ	charge carrier mobility
$Mo(tfd)_3$	molybdenum tris(1,2-bis(trifluoromethyl)ethane-1,2-dithiolene)
n	charge carrier density

N-DMBI	4-(2,3-Dihydro-1,3-dimethyl-1H-benzimidazol-2-yl)-*N*,*N*-dimethylbenzenamine
N-DPBI	4-(1,3-Dimethyl-2,3-dihydro-1H-benzoimidazol-2-yl)-*N*,*N*-diphenylaniline
NDI	naphthalene diimide
NIR	near-infrared
OECT	organic electrochemical transistor
OFET	organic field-effect transistor
OLED	organic light-emitting diode
p($g_4$2T-T)	thiophene based copolymer with oligoethylene glycol side chains
p($g_4$2T-TT)	thienothiophene based copolymer with oligoethylene glycol side chains
p(gNDI-gT2)	naphtalene diimide dithiophene copolymer with oligoethylene glycol based side chains
p(NDI2OD-T2)	naphtalene diimide dithiophene copolymer, also N2200
P3HT	poly(3-hexylthiophene-2,5-diyl)
pBTTT	poly[2,5-bis(3-tetradecylthiophen-2-yl)thieno[3,2-b]thiophene]
PCBM	[6,6]-phenyl-C_{61}-butyric acid methyl ester
PDI	perylene diimide
PEDOT	poly(3,4-ethylenedioxythiophene)
PEI	poly(ethylene imine)
PEO	poly(ethylene oxide)
PE	polyethylene
PLLA	poly(L-lactic acid)
PPV	poly(p-phenylene vinylene)
PS	polystyrene
PSS	poly(styrene sulfonate)
q	elementary charge
σ	electrical conductivity
TDAE	tetrakis(dimethylamino)ethylene
TOS	p-toluenesulfonic acid
UPS	ultraviolet photoelectron spectroscopy
UV-vis	ultraviolet-visible
ZT	thermoelectric figure of merit at temperature T

List of publications

This thesis consists of an extended summary and the following appended papers:

Paper I

A Solution-Doped Polymer Semiconductor:Insulator Blend for Thermoelectrics.
David Kiefer, Liyang Yu, Erik Fransson, Andrés Gómez, Daniel Primetzhofer, Aram Amassian, Mariano Campoy-Quiles, Christian Müller
Advanced Science, **2017**, *4*, 1600203.

Paper II

Polar Side Chains Enhance Processability, Electrical Conductivity, and Thermal Stability of a Molecularly p-Doped Polythiophene.
Renee Kroon, David Kiefer, Dominik Stegerer, Liyang Yu, Michael Sommer, Christian Müller
Advanced Materials, **2017**, *29*, 1700930.

Paper III

Enhanced n-Doping Efficiency of a Naphthalenediimide-Based Copolymer through Polar Side Chains for Organic Thermoelectrics.
David Kiefer, Alexander Giovannitti, Hengda Sun, Till Biskup, Anna I. Hofmann, Marten Koopmans, Camilla Cendra, Stefan Weber, L. Jan Anton Koster, Eva Olsson, Jonathan Rivnay, Simone Fabiano, Iain McCulloch, Christian Müller
ACS Energy Letters, **2018**, *3*, 278–285.

Paper IV

Double Doping of Conjugated Polymers with Monomer Molecular Dopants.
David Kiefer, Renee Kroon, Anna I. Hofmann, Hengda Sun, Xianjie Liu, Alexander Giovannitti, Dominik Stegerer, Alexander Cano, Jonna Hynynen, Liyang Yu, Yadong Zhang, Dingqi Nai, Thomas F. Harrelson, Michael Sommer, Adam J. Moulé, Martijn Kemerink, Seth R. Marder, Iain McCulloch, Mats Fahlman, Simone Fabiano, Christian Müller
Nature Materials, **2019**, *18*, 149-155.

Related publications not included in the thesis:

Paper A

Increasing the Thermoelectric Power Factor of a Semiconducting Polymer by Doping from the Vapor Phase.
Shrayesh N. Patel, Anne M. Glaudell, David Kiefer, Michael L. Chabinyc
ACS Macro Letters, **2016**, *5*, 268-272.

Paper B

Thermoelectric Plastics: from Design to Synthesis, Processing and Structure-Property Relationships.
Renee Kroon, Desalegn A. Mengistie, David Kiefer, Jonna Hynynen, Jason D. Ryan, Liyang Yu, Christian Müller
Chemical Society Reviews, **2016**, *45*, 6147-6164.

Paper C **Bulk Doping of Millimeter-Thick Conjugated Polymer Foams for Plastic Thermoelectrics.**
Renee Kroon, Jason D. Ryan, David Kiefer, Liyang Yu, Jonna Hynynen, Eva Olsson, Christian Müller
Advanced Functional Materials, **2017**, *27*, 1704183.

Paper D **Enhanced Electrical Conductivity of Molecularly p-Doped Poly(3-hexylthiophene) through Understanding the Correlation with Solid-State Order.**
Jonna Hynynen, David Kiefer, Liyang Yu, Renee Kroon, Rahim Munir, Aram Amassian, Martijn Kemerink, Christian Müller
Macromolecules, **2017**, *50*, 8140–8148.

Paper E **Influence of Crystallinity on the Thermoelectric Power Factor of P3HT Vapour-Doped with F4TCNQ.**
Jonna Hynynen, David Kiefer, Christian Müller
RSC Advances, **2018**, *8*, 1593–1599.

Contribution Report

Paper I Main author. Experimental design and preparation of all samples. Electrical, thermal, optical and mechanical measurements. Data analysis and interpretation. Compiled the data for and wrote most of the paper.

Paper II Shared main author. Solution processing and preparation of (doped) polymer samples. Optical spectroscopy, electrical, thermal, GIWAXS measurements and fitting of UV-vis spectra. Data analysis and interpretation. Compiled data for and wrote a significant part of the paper.

Paper III Main author. Solution processing and preparation of all samples. Optical spectroscopy and thermal stability measurements. Data analysis and interpretation. Electrical measurements together with H.S. Compiled data for and wrote most of the paper.

Paper IV Main and corresponding author. Experimental design, solution processing and preparation of all samples. Optical spectroscopy, electrical measurements and fitting of UV-vis spectra. Measurement and analysis of GIWAXS. Compiled data for and wrote most of the paper.

Contents

1 Introduction

The demonstration of the first transistor in the 1940s marked the starting point for the era of electronics.[1] Since then, electronics have become an omnipresent part of everyday life, for example, in the form of personal devices such as computers and mobile phones. The class of materials, which enables all types of electronic technology, are *semiconductors*. Today, electronics are mostly based on inorganic semiconductors, such as silicon or gallium arsenide. Instead, electronics can also be built with organic semiconductors, a particular type of molecules that can conduct electricity. They are particularly attractive for their potential low-cost manufacture and mechanical flexibility. The field of organic electronics received its critical spark in the mid-1970s by the discovery of metal-like conductivity in the π-conjugated polymer polyacetylene achieved by oxidation with iodine vapour.[2] Over the years this led to further revelations such as electroluminescence in small molecules[3] and conjugated polymers[4] and the demonstration of photovoltaic cells based on organic molecules.[5–7] In the year 2000, more than two decades after the discovery was made, the dawn of organic electronics was recognized with the Nobel prize in Chemistry for Alan Heeger, Alan MacDiarmid and Hideki Shirakawa.[8]

Today, the (potential) application areas of organic electronics range from display technology and lighting applications, energy harvesting and storage to bioelectronics. Electronics based on organic materials offer the benefit of uncomplicated, high-throughput and low-temperature manufacturing, by e.g. roll-to-roll printing, and the ability to tailor their chemical structure for specific optical and electronic properties.[9] A prominent example of commercial products based on organic semiconductors are organic light-emitting diodes (OLEDs). They have become a key technology for displays in smartphones and high-end TV screens because of to the broad spectrum of colours and better contrast that can be realised with organic semiconductors compared with inorganic alternatives.[10] Other

commercial products for OLED technology include flexible decorative lighting panels and car taillights.[11,12] Organic field-effect transistors (OFETs) are another type of device that were introduced for flexible e-paper displays[13] and have been demonstrated for use as sensors[14] and switching circuits.[15]

Organic solar cells are deemed a possible alternative to silicon solar cells, that are potentially semi-transparent and may be printed on flexible substrates.[16] Organic thermoelectric generators are another energy harvesting technology that is widely studied. They allow direct conversion of heat into electrical energy or vice versa to make use of waste heat or for cooling/heating.[17,18] The compelling ability of some organic semiconductors to conduct both electronic and ionic charges can be used for organic batteries or capacitors[19] and more recently as an interface to the biological world, explored within the field of organic bioelectronics.[20,21]

Organic semiconductors come in a vast structural variety that influences their properties and enables customisation for specific applications. Generally, organic semiconductors can be categorized into small molecular and polymeric semiconductors, i.e. conjugated polymers. Small molecular semiconductors are polycyclic aromatic hydrocarbons, such as pentacene (figure 1.3). Conjugated polymers on the other hand feature extended π-conjugated systems, e.g. along their backbones. Other carbon-based semiconductors are fullerenes (figure 1.3), as well as graphene and carbon nanotubes, which comprise single sheets or tubes of hexagonal carbon atoms, respectively.[22] This thesis will focus on conjugated polymers, which will be discussed in more detail during the following section.

1.1 Conjugated Polymers

Polymers are molecules with relatively high molecular mass (macromolecules) that consist of repeat units, which are "derived, actually or conceptually, from molecules of low relative molecular mass".[23] The majority of polymers, such as polyolefins, are insulators since they feature a band gap >5 eV. Instead, conjugated polymers, such as polyacetylene (figure 1.3), are semiconductors with a band gap <3 eV because of π-conjugation, which is the result of alternating double bonds between unsaturated carbon atoms. Double bonds are formed by the four valence electrons of a carbon atom. One electron is dedicated to the σ-bond between sp^2 orbitals and a second electron to the π-bond by the overlap of p-orbitals (figure 1.1). Since the chemical structure is maintained by the σ-electrons, π-electrons can undergo electronic transitions induced by e.g. light or redox reactions.

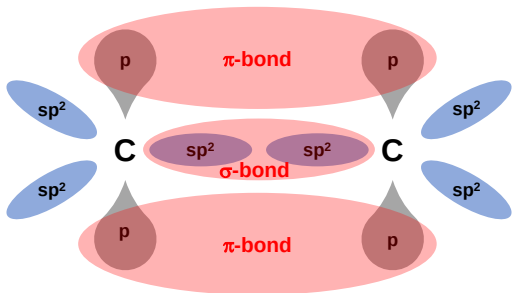

Figure 1.1: *Schematic of double bond formation between two carbon atoms by the overlap of sp^2- and p-orbitals.*

Energy level splitting for π-bonds leads to a bonding π- and an anti-bonding π*-orbital, which constitute the highest occupied molecular orbital (HOMO) and the lowest unoccupied molecular orbital (LUMO), respectively. The band gap (E_g) of a conjugated polymer is the difference between its HOMO and LUMO energy. Alternating single and double bonds form a π-conjugated system over which the π-electrons are delocalized. The band gap of an organic semiconductor reduces with the extent of conjugation as a

result of progressive energy band splitting (figure 1.2) leading to more semiconducting properties.

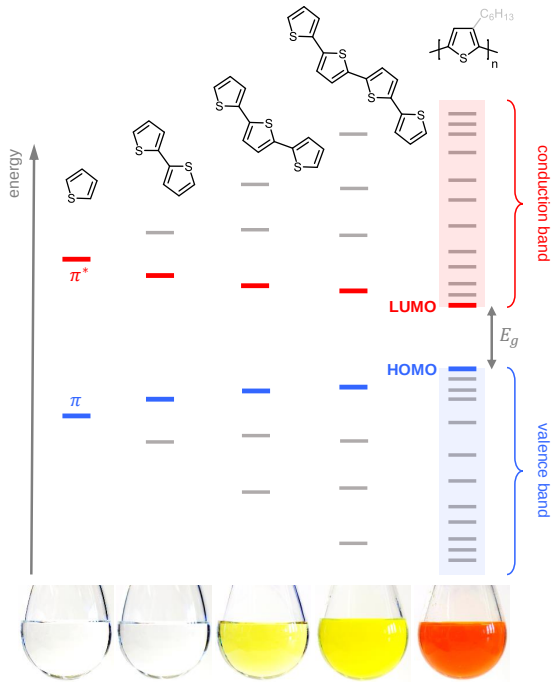

Figure 1.2: *Evolution of the HOMO and LUMO levels as well as the band gap* E_g *with increasing number of thiophene repeat units, resulting in valence and conduction bands for polythiophene. Reproduced from reference* 17 *with permission from the Royal Society of Chemistry.*

Conjugated polymers commonly feature a band gap between 1.5 and 3 eV, which is considerably larger compared with a band gap <1.1 eV for conventional inorganic semiconductors. Therefore, the intrinsic charge carrier density in conjugated polymers at room temperature is relatively low and requires generation of charge carriers by external stimuli, such as absorption of light or molecular doping. Doping either induces negative (n-type) charge carriers by the addition of electrons or positive (p-type) charge carriers by the

removal of electrons, i.e. formation of holes, and will be covered in more detail in chapter 2.

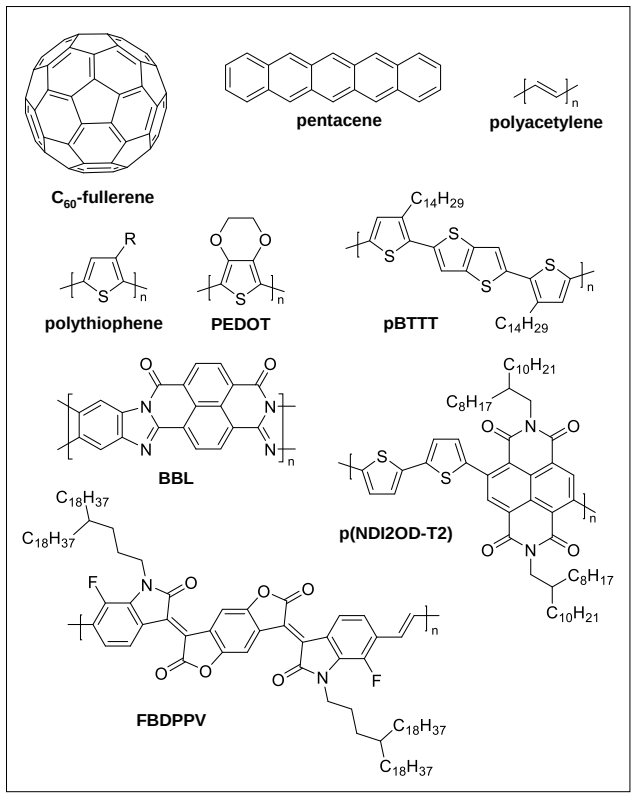

Figure 1.3: *Chemical structures of some small molecular and polymer semiconductors.*

The properties of conjugated polymers can be influenced by a wide set of tools, such as synthetic methods to change their chemical structure or manipulation of their solid-state properties by the choice of processing method. For example, the choice of repeat unit directly influences the optoelectronic properties of a conjugated polymer.[24,25] The polythiophene poly(3-hexylthiophene-2,5-diyl) (P3HT) consist of only one type of repeat unit and behaves as a p-type semiconductor. Instead, the donor-acceptor polymer p(NDI2OD-T2) comprising alternating donor dithiophene and acceptor naphtalene diimide (NDI) units is characterised as n-type. Co-polymerisation of donor and acceptor units is a general

tool to reduce the band gap of a conjugated polymers, which is beneficial for e.g. organic solar cells.

Since unsubstituted conjugated polymers such as polythiophene are intractable, solubility in organic solvents is usually enabled by aliphatic side chains. Side chains also facilitate synthesis of high molecular weight conjugated polymers. The length and regularity of alkyl side chains has a strong influence on the thermal properties such as the melting and glass-transition temperature.[26,27] Moreover, side chain design can be used to adjust other physical properties, such as light absorption and charge transport, as well as interactions with ions.[28] The specific case of oligoethylene glycol side chains will be discussed in this thesis (cf. Section 3.2).

Semi-crystalline conjugated polymers, such as regioregular P3HT, have the ability to form ordered structures, which significantly influence its optoelectronic properties. Crystallisation is influenced by the molecular structure as well as the choice of processing schemes, such as solvent and casting temperature. Higher charge carrier mobilities are also achieved by a more rigid backbones like in the case of poly[2,5-bis(3-tetradecylthiophen-2-yl)thieno[3,2-b]thiophene] (pBTTT).[29]

2 Molecular Doping of Conjugated Polymers

Organic semiconductors in their pristine (undoped) state feature no intrinsic charge carriers. Therefore doping is used to introduce and control the desired amount of charges in organic semiconductors, e.g. for certain layers in thin film devices (cf. section 2.3), such as OLEDs, OFETs and organic solar cells,[30,31] or bulk applications, like organic thermoelectrics[18] and conducting fibres.[32] For conventional inorganic semiconductors the term "doping" refers to small impurities of atoms that have a lower or higher valence in the host semiconductor.[33] Instead, organic semiconductors are doped by addition of dopant molecules (atoms) or transition metal complexes. This process is commonly referred to as *molecular doping* and the result of p- or n-doping are positive or negative charges, respectively. This thesis will focus on molecular doping of conjugated polymers. Molecular doping is also used for charge carrier density modulation in e.g. small molecule semiconductors,[31] carbon nanotubes and graphene,[22] as well as perovskites[34] and quantum dots[35], which will not be covered here.

2.1 Basic Principles

The two prevalent mechanisms to achieve molecular doping are acid/base or redox doping (figure 2.1). Acid/base doping entails a chemical reaction by the transfer of a hydride H^- for n-doping and a proton H^+ in case of p-doping from the neutral dopant molecule to the semiconductor.[33,36] The charge neutrality is maintained by the reacted dopant molecule acting as counter-ion for the charge on the semiconductor. In case of redox doping, strong electron accepting (p-doping) or electron donating (n-doping) molecules are added to the semiconductor.[37,38] The result is a charge pair, which can be a charge transfer complex or an ion pair provided that full charge transfer occurs (figure 2.4). The

ionisation energy (IE) and electron affinity (EA) of the donor and acceptor should be similar in order for efficient charge transfer to occur. Redox doping is further discussed in the next section and chapter 4. A third mechanism is doping with Lewis acids and bases that can coordinate to the semiconductor with their electrophilic or nucleophilic centre and induce charge carriers by a redistribution of the electron density[39,40] or through an anion assisted electron transfer.[41,42]

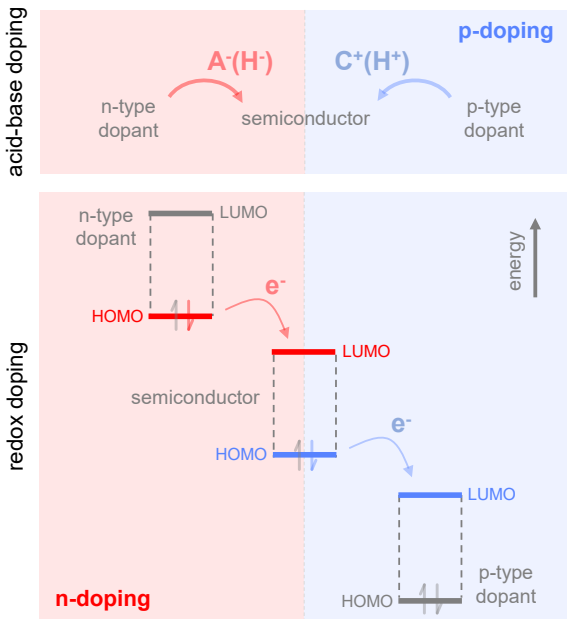

Figure 2.1: *Basic principle of acid/base doping, which involves the transfer of an anion (A^-, typically H^-) or cation (C^+, typically H^+) to the semiconductor (top); and redox doping, which involves the transfer of an electron to the LUMO or from the HOMO of the semiconductor in the case of n- and p-doping, respectively (bottom). Adapted from reference 17 with permission from the Royal Society of Chemistry.*

A radical cation (radical anion), i.e. a polaron, is formed in the case of p-doping (n-doping), that is delocalized over several repeat units, and is associated with changes of the local electronic structure as shown exemplary for p-doping in figure 2.2. In a traditional model the HOMO and LUMO levels are shifted away from the valence and conduction band,

into the band gap, resulting in additional absorption bands in the optical spectra of the polymer.[43] Very recently a revised set of models was proposed that reconsidered the Coulomb interactions inside the doped semiconductor, which is thought to cause splitting of the HOMO level.[44–47] Thus, the remaining unpaired electron lies energetically below the valence band edge, which is consistent with the prevailing observation that the IE of p-doped semiconductors is increased. Although polaron formation is favoured, dications (dianions), i.e. bipolarons, may form at high doping levels.

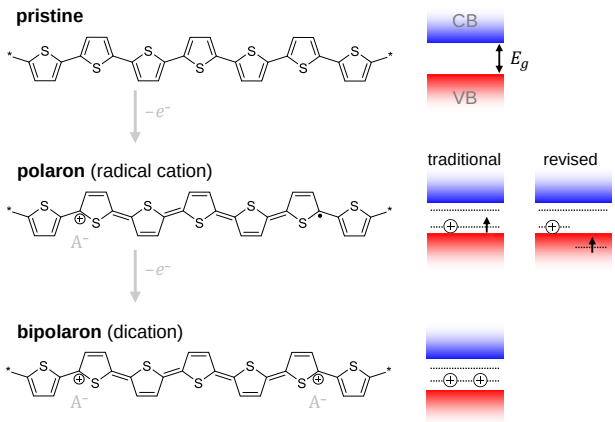

Figure 2.2: *Schematic for p-doping of polythiophene (left) and corresponding band structure (right). Upon removal of an electron (e^-) from the pristine polymer (top) a polaron (middle) is formed; traditional model: HOMO and LUMO are shifted away from band edges, revised model: HOMO level is split with remaining electron below the valence band edge. At high doping levels bipolarons may form by removal of a second electron (bottom). The electron acceptor acts as negative counterion (A^-) to the positive charges.*

2.1.1 Dopant Molecules

A large variety of molecular p- and n-dopants (figure 2.3) featuring different chemical structures, working mechanisms and purposes exist. This section will provide a brief overview over different dopants and the specific ones used in this thesis.

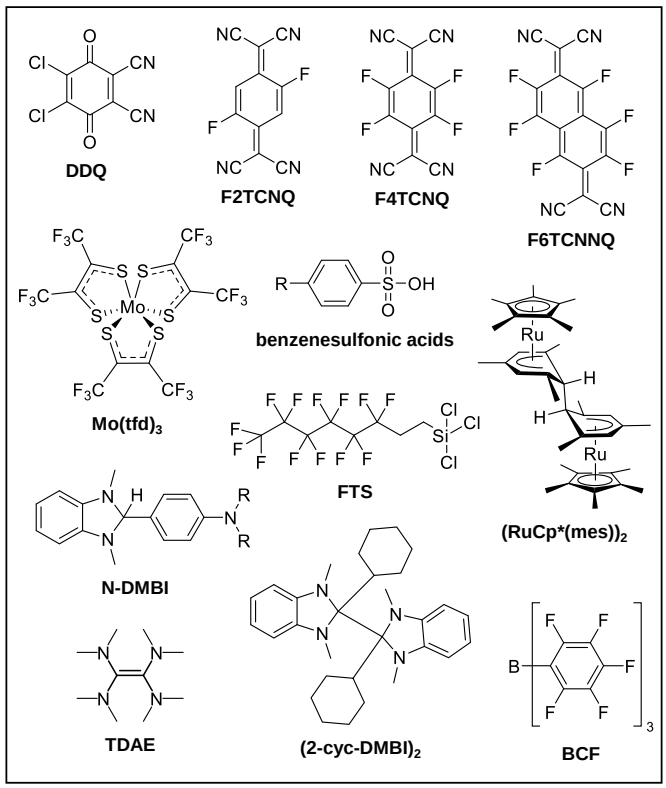

Figure 2.3: *Chemical structures of common p- and n-dopants. 2,3-dichloro-5,6-dicyano-1,4-benzoquinone (**DDQ**), 2,5-difluoro-7,7,8,8-tetracyanoquinodimethane (**F2TCNQ**), 2,3,5,6-tetrafluoro-7,7,8,8-tetracyanoquinodimethane (**F4TCNQ**), 1,3,4,5,7,8-hexafluoro-tetracyanonaphthoquinodimethane (**F6TCNNQ**), molybdenum tris(1,2-bis(trifluoromethyl)ethane-1,2-dithiolene) (**Mo(tfd)$_3$**), **benzene sulfonic acids**, 4-(2,3-Dihydro-1,3-dimethyl-1H-benzimidazol-2-yl)-N,N-dimethylbenzenamine (**N-DMBI**), (tridecafluoro-1,1,2,2-tetrahydrooctyl)trichlorosilane (**FTS**), dimeric ruthenium sandwich compound (**(RuCp*(mes))$_2$**), tetrakis(dimethylamino)ethylene (**TDAE**), DMBI dimer (**(2-cyc-DMBI)$_2$**), Tris(pentafluorophenyl)borane (**BCF**)*

p-Dopants

Early examples of redox doping of conjugated polymers are doping with iodine vapor (I_2)[2] or iron chloride ($FeCl_3$)[48] solutions. Doping of stretch-aligned polyacetylene with I_2 was found to result in a very high electrical conductivity of $6 \times 10^5\,S\,cm^{-1}$,[49] but unfortunately features a low stability.[50] A particular focus in this thesis lies on doping with strong electron acceptors based on quinone cores that feature high EAs such as F4TCNQ (5.2 eV) and various other common analogues with either higher (e.g. F6TCNNQ, 5.3 eV[51]) or lower EA (e.g. DDQ, 4.6 eV[52]; F2TCNQ, 5.1 eV[51]). Examples of F4TCNQ doped polymers include polyfluorenes,[53,54] thiophene-based polymers, like P3HT[55–61] and pBTTT,[62–65] as well as DPP-based polymers.[66,67] In particular doping of P3HT with F4TCNQ, a model system for molecular doping, was covered by many recent studies that investigated the doping mechanism,[55–58,60,61,68] the effects of processing techniques[69–73] and structure-property relationships.[68,74–76]

The interaction between redox dopants and conjugated polymers are described by either integer charge transfer, that is the formation of an ion pair, or fractional charge transfer by the formation of a charge transfer complex through hybridisation of the molecular orbitals (figure 2.4). Fractional charge transfer requires thermal ionization to create charge carriers, and is thus considered limiting for the electrical performance. Whether a charge transfer complex or an ion pair is formed between a semiconductor and a dopant depends on the overlap between molecular orbitals of the dopant and semiconductor,[61,68,77–79] the charge distribution in the semiconductor[80–82] and the dopant strength[38,83] (refer to chapter 4 for further discussion).

In case of P3HT and F4TCNQ ion pair formation is most commonly observed. However, Jacobs *et al.* recently showed that the extent of charge transfer between P3HT and F4TCNQ strongly depends on the crystalline structure of the doped conjugated polymer. The authors reported a specific processing-dependent polymorph of F4TCNQ:P3HT that

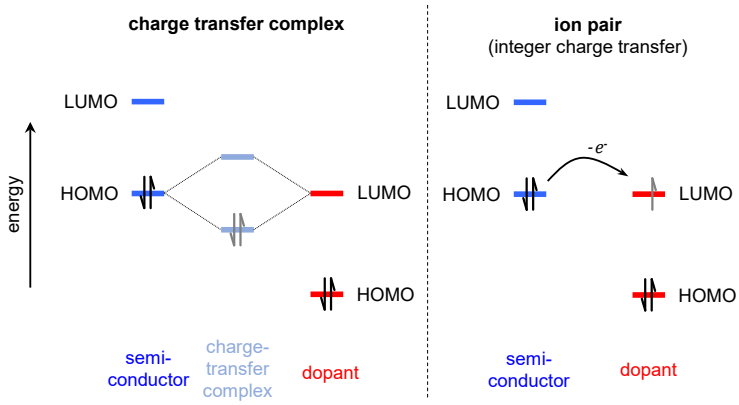

Figure 2.4: *Formation of a charge transfer complex through fractional charge transfer by intermolecular hybridisation between the semiconductor and the dopant (left) and formation of an ion pair involving the transfer of an electron (e^-) from the semiconductor to the dopant (right); both cases for p-doping. Charge transfer complexes require thermal ionisation in order to form charge carriers and hence lower carrier concentrations and electrical conductivities are observed compared with ion pairs.*

only exhibits partial charge transfer, which could be converted to integer charge transfer by post-treatment with solvent.[68] Mendez *et al.* showed that the oligomer quaterthiophene (4T) with the same backbone as P3HT only results in fractional charge transfer, which was ascribed to the different packing in F4TCNQ:4T charge transfer crystallites compared with F4TCNQ-doped P3HT. Other examples of strongly oxidising charge transfer dopants are soluble molybdenum dithiolene complexes[84] that have been shown to dope P3HT,[85,86] as well as benzo-dithiophene-[87,88] and DPP-based polymers.[89]

An example for the protonation of polymers such as polythiophenes[90,91] and polyaniline[92] are strong organosulfuric acids, e.g. benzenesulfonic acids, or sulfonic acid groups in the side chains of self-doped polymers.[28,93,94] The doping ability of acids is correlated with the strength of the acid and is thought to be further enhanced by an acid-mediated oxygen doping mechanism.[36,95,96] Acid doping is also achieved with a perfluorinated silane (FTS),

which proceeds through the hydrolysis of the silane and subsequent protonation of the polymer.[91] In case of PEDOT:PSS or PEDOT:TOS, which are of interest particularly for organic thermoelectrics[97,98] or organic bioelectronics,[99] the polyacid poly(styrene sulfonate) (PSS) or p-toluenesulfonic acid (TOS), counterbalance the charges in PEDOT that is already synthesised in its oxidised form. A third type of dopant are Lewis acids such as the borane dopant BCF, which was shown to dope P3HT[100] and an indenopyrazine-based polymer that cannot be doped by F4TCNQ.[101]

n-Dopants

Air-stable benzimidazole compounds like N-DMBI or N-DPBI are effective n-dopants for conjugated polymers, like PPV-,[102] NDI-,[103,104] DPP-based polymers,[105,106] the ladder type polymer BBL[107] and fullerenes.[108,109] Doping with N-DMBI, which is used as the n-dopant in this thesis, is thought to proceed through the transfer of a hydride to the semiconductor, which may be followed by additional charge transfer events.[108] More recently dimers of DMBI were demonstrated as efficient n-dopants, which instead of hydride transfer work through dimer splitting into two radicals followed by electron transfer.[104,110,111] Other air-stable dimer dopants are based on organometallic sandwich compounds like $(RuCp^*(mes))_2$,[112–114] able to n-dope e.g. DPP based polymers.[115]

N-doping can also be realized with the powerful reducing agent TDAE, used to reduce PEDOT:TOS[116] and to dope fullerenes,[117,118] as well as NDI and ladder-type polymers.[107,119] A further example are amine functionalities like small molecular impurities of the polymer poly(ethylene imine) (PEI),[120,121] self-doped/self-compensated fullerene derivatives,[122] PDI derivatives[123] and PPV-based polymers.[124,125] Moreover, tertiary ammonium salts were recently demonstrated as dopants for fullerene derivatives[126] and DPP polymers.[41,42]

2.2 Dopant Processing Methods

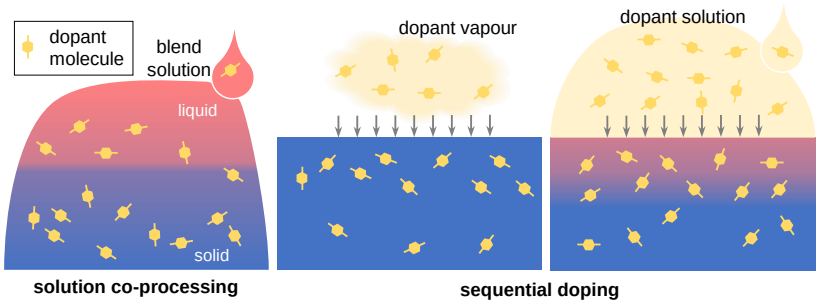

Figure 2.5: *Schematic of solution co-processing (left) and sequential doping by dopant vapour (middle) and solution (right).*

The choice of processing method is an important parameter which has a strong influence on the efficiency of the doping process and the formation of the final nanostructure of a doped polymer. In general, two processing schemes exist that permit doping of conjugated polymers (figure 2.5). Solution co-processing is a simple one-step doping process, which entails the dissolution of polymer and dopant in the same or compatible solvents, admixing at appropriate proportions followed by removal of the solvent. Benefits, like the simplicity and exact control over the amount of incorporated dopant, are often met with issues of the processability due to dopant:polymer interactions leading to precipitation or phase-separation during film formation. The result is often an unfavourable nanostructure, which gives rise to only limited electrical performance, like in the case of P3HT co-processed with F4TCNQ.[57,69] To mitigate these problems the dopant can instead be applied through sequential doping, i.e. by exposure of the solidified conjugated polymer to a solution of the dopant in an orthogonal solvent,[69,70,91] or dopant vapour.[64,65,74] In fact, the latter method was used by Shirakawa *et al.* in their seminal study of iodine vapour-doped polyacetylene (cf. chapter 1).[2] Sequential doping allows control over the polymer nanostructure formation prior to the introduction of the dopant, which eliminates effects

due to possible dopant:semiconductor interaction in solution.[74,127] On the the other hand, an additional processing step needs to be performed and dopant molecules have to diffuse through the semiconductor, which can be a limiting factor for doping of thick bulk structures.[128] Thick bulk structures may also be achieved with sequential doping of conjugated polymer foams.[128]

2.3 Importance of Molecular Doping for Organic Electronics

The concept of molecular doping is widely utilized. For instance, OLEDs and organic solar cells contain interlayers, i.e. charge transporting, blocking or injection/extraction layers, which are carefully tuned to achieve the desired type and density of charge carriers (n- or p-type) or to match the energy levels of the active layers and electrodes in order to minimize contact resistance and avoid injection barriers.[129] Also the active, emissive layer in OLEDs and the bulk-heterojunction layers in solar cells can benefit from molecular doping.[130,131] In transistors doping can be used to passivate traps or to define the majority type of charge carrier.[31] Additionally, the contact layers in OFETs can benefit from doping and improve charge injection and transport. Doping is also needed in the case of bulk materials, such as conducting fibres and yarns for e.g. triboelectric or piezoelectric textiles.[32] One topic which currently attracts considerable interest is organic thermoelectrics for waste heat recovery, low-temperature energy harvesting or point cooling/heating. The requirements for the electrical conductivity of doped components differ depending on the specific use. For example, trap-filling with minute amounts of dopants does not significantly modify the electrical conductivity, but facilitates better transport of charges in e.g. transistors. Instead, injection layers require an electrical conductivity that is as high as possible to enable efficient contacts. Organic thermoelectric devices require both efficient n- and

p-type materials (figure 2.6) and comprise a particular challenge because of a number of interdependent parameters that need to be considered simultaneously.[17,18,132] Therefore, molecular doping of conjugated polymers will be discussed in more detail in the context of organic thermoelectrics.

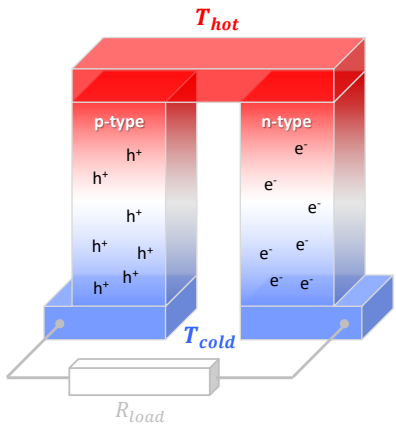

Figure 2.6: *Thermoelectric element comprising an n-type and a p-type leg, which are connect thermally in parallel and electrically in series. The legs experience a temperature gradient* $\Delta T = T_{hot} - T_{cold}$ *resulting in the diffusion of charge carriers towards the cold ends. Reproduced from reference 17 with permission from the Royal Society of Chemistry.*

Conducting and semiconducting materials, which are exposed to a temperature gradient (ΔT) will experience the Seebeck effect, i.e. the diffusion of charge carriers towards the cold end resulting in a measurable electrical potential (ΔV) along the temperature gradient. The Seebeck effect, which can be regarded as the entropy per charge carrier, is described by the Seebeck coefficient, $\alpha = -\Delta V/\Delta T$. The sign of the Seebeck coefficient denotes the majority type of charge carrier, that is negative fore n-type and positive for p-type, and its absolute value is desired to be as large as possible in order to maximize the voltage output. At the same time the electrical conductivity (σ), given by the product of the elementary charge (q), the charge carrier density (n) and mobility (μ), i.e. $\sigma = qn\mu$, should be high to minimize losses by joule heating. A third criterion is a low thermal conductivity ($\varkappa$), which

is required to maintain the temperature gradient and is comprised of contributions from phonons and charge carriers. The electric contributions to the thermal conductivity is often omitted for organic materials due to the low charge carrier concentrations in organic semiconductors, and thus, their thermal conductivity is often considered as constant. The thermoelectric figure of merit ZT, the key performance indicator for thermoelectric materials at a given temperature T, links all three parameters:

$$ZT = \frac{\alpha^2 \sigma}{\varkappa} T \tag{2.1}$$

If $\varkappa$ is unknown the thermoelectric power factor, i.e. $\alpha^2\sigma$, is commonly used to compare materials instead.

Introduction of charge carriers by doping of a semiconductor, required to increase its electrical conductivity, is unfortunately concomitant with a drop of the Seebeck coefficient. Additionally, at high charge carrier concentrations the thermal conductivity will rise due to its electronic component. Hence, the optimization requires a compromise between the different parameters. In case of traditional inorganic thermoelectric materials this is displayed in an optimal charge carrier concentration below and above which their performance decreases. Instead, in conjugated polymers an optimum charge carrier concentration has not yet been observed due to persistent low charge carrier concentrations in organic materials.

A few examples of recent literature values for p- and n-type organic thermoelectric materials based on conjugated polymers are listed in table 2.1. Currently, some of the best performing p-type materials are based on highly oxidized PEDOT that was post-treated to tune the oxidation level or to remove insulating PSS.[116,133] For example Bubnova *et al.* chose to carefully optimise the electrical conductivity and Seebeck coefficient of PEDOT:Tos by dedoping with TDAE reaching a high power factor of $324\,\mu W\,m^{-1}\,K^{-2}$ and a thermoelectric figure of merit ZT of 0.25.[116] Similarly high ther-

moelectric performance was also achieved by dedoping with hydrazine[134] or oxidation with bis(trifluoromethylsulfonyl)imide.[135]

Table 2.1: *Examples of thermoelectric p- and n-doped conjugated polymers (see figure 1.3 for polymer structures).*

polymer	dopant/counterion	σ [a]	α [b]	$\alpha^2\sigma$ [c]	$\varkappa$ [d]	ZT [e]	ref.
PEDOT	Tos + TDAE	70	215	324	0.37	0.25	[116]
pBTTT	F4TCNQ	670	42	70	-	-	[65]
FBDPPV	N-DMBI	6	-213	27	-	-	[106]
BBL	TDAE	1.7	-60	0.6	-	-	[107]

[a] $[\mathrm{S\,cm^{-1}}]$ [b] $[\mu\mathrm{V\,K^{-1}}]$ [c] $[\mu\mathrm{W\,m^{-1}\,K^{-2}}]$ [d] $[\mathrm{W\,m^{-1}\,K^{-1}}]$ [e] at r.t.

The thermoelectric properties of doped solution-processable conjugated polymers like P3HT and pBTTT have also been studied intensively. Many recent studies focus on increasing the electrical conductivity by understanding the impact of different dopants and their processing methods[63,91] as well as the impact of the semiconductor nanostructure.[65,75,136] For example, Glaudell *et al.* compared the electrical conductivities and Seebeck coefficients of a set of conjugated polymers doped with F4TCNQ and FTS and derived an empirical correlation,[63] which in fact is now commonly used for assessing the thermoelectric performance of doped conjugated polymers. Other studies have focused on the chemical structure of the side chains to improve doping for thermoelectrics.[28,51,137,138] For example the polymer PQTS12, a polythiophene with thioalkyl side chains was found to exhibit a moderate Seebeck coefficient of $\sim$16 $\mu\mathrm{V\,K^{-1}}$ and a high electric conductivity of $\sim$350 $\mathrm{S\,cm^{-1}}$ after doping with nitrosonium tetrafluoroborate ($NOBF_4$).[137] In another study, sequential doping of pBTTT by F4TCNQ vapour permitted to study the effect of the molecular order of the polymer. Highly ordered pBTTT films were found to exhibit the highest electrical conductivity reaching 670 $\mathrm{S\,cm^{-1}}$ and a corresponding large Seebeck coefficient of 42 $\mu\mathrm{V\,K^{-1}}$ resulting in a power factor of 70 $\mu\mathrm{W\,m^{-1}\,K^{-2}}$.[65] Other examples include doping of semiconducting polymer blends[139–141] or aligned polymer films,[76,86]

which is a promising avenue to increase the electrical conductivity without sacrificing the Seebeck coefficient.

Organic n-type materials are generally harder to realize as a result of the instability of their n-doped state in ambient environment.[142] Their performance continues to lag behind that of p-type materials. However, recently high electrical conductivities and high thermoelectric power factors for several doped n-type conjugated polymers were reported.[42,106,143] An early example includes the high-mobility n-type polymer p(NDI2OD-T2) doped with N-DMBI, which can reach an electrical conductivity of $3 \times 10^{-3}\,\mathrm{S\,cm^{-1}}$ despite strong phase-separation inside dopant:semiconductor films.[103] The same dopant was used to dope the DPP-based polymer FBDPPV achieving a high electric conductivity of $6\,\mathrm{S\,cm^{-1}}$ with a corresponing Seebeck coefficient of $-213\,\mu\mathrm{V\,K^{-1}}$ and a record-high thermoelectric power factor for organic n-type materials of $27\,\mu\mathrm{W\,m^{-1}\,K^{-2}}$.[106] Another example is the ladder-type polymer BBL that doped with TDAE vapour reached an electrical conductivity of $1.7\,\mathrm{S\,cm^{-1}}$.[107] Excitingly, n-doping of the thionated NDI thiophene copolymer 2S-*trans*-PNDIT2 with N-DPBI results in an air-stable n-doped state as a result of the low EA of the polymer as reported by Nava *et al.*[144] The n-doped polymer displayed a conductivity of $6 \times 10^{-3}\,\mathrm{S\,cm^{-1}}$ and a Seebeck coefficient of $-90\,\mu\mathrm{V\,K^{-1}}$. Air-stability of n-doped conjugated polymers will be further discussed in chapter 5.2.

Overall, some major challenges for efficient doping of conjugated polymers remain. For both p- and n-doped conjugated polymers ways to decrease the required volume fraction of dopant are needed to allow preservation of the semiconductor nanostructure after doping. Further, the thermal stability of the doped state needs to be improved especially in the context of organic thermoelectrics, where elevated temperatures up to 200 °C may be reached. The air-stability of n-doping requires additional attention, in order to realise durable thermoelectric modules comprising both p- and n-type legs.

2.4 Aims of the Thesis

This thesis aims to investigate the following research questions:

- Can the processability/miscibility of conjugated polymers and molecular dopants be improved by blending with more polar insulator polymers or exchange of aliphatic with polar side chains? (chapter 3)
- Can the efficiency of molecular p-doping be improved lowering the ionisation energy of conjugated polymers? (chapter 4)
- How is the thermal stability of p-doped and the air stability of n-doped conjugated polymers affected by polar side chains? (chapter 5)

3 Compatibility & Solubility

Conjugated polymers are promising materials for high-throughput solution printing and coating techniques, which can enable low-cost flexible electronics. Organic devices, such as solar cells and transistors, consist of layers that need to be applied in individual processing steps. One way that is widely used to achieve doped layers for e.g. OLEDs is co-evaporation of semiconductors and dopants, which is, however, limited to small molecular semiconductors due to the inability of polymers to evaporate. Thus, to realize layers of doped conjugated polymers in a single step, semiconductors and molecular dopants must be processed from the same solution. However, several issues with co-processing persist, such as the lack of co-solvents,[52,138] agglomeration of semiconductor and dopant in solution[69,70,145] and the impact of the molecular dopant on the polymer nanostructure that forms during solidification, which is known to influence the electrical performance.[57,88,103] Sequential doping, by diffusion of the dopant into the previously solidified semiconductor (chapter 2.2), is one avenue to avoid co-processing, but would add an additional processing step and is not suitable for bulk structures that are needed for e.g. thermoelectrics.

Ways that mitigate processing issues and reduce the required amount of dopant are highly desired. One often encountered challenge is the poor compatibility between typically non-polar conjugated polymers and polar molecular dopants. For example, P3HT and F4TCNQ are known to aggregate when co-processed from chlorinated solvents due to the formation of an insoluble ion pair, which can be dissociated by heating of the solution.[60] Unfortunately, films prepared at elevated temperatures display reduced electrical performance caused by domains of unreacted dopant molecules that interrupt the semiconductor nanostructure. Consequently, a low electrical conductivity of typically not more than $1\,\mathrm{S\,cm^{-1}}$ is measured for films of P3HT or pBTTT co-processed with F4TCNQ.[57,60,63] Likewise, films of

p(NDI2OD-T2) co-processed with the n-dopant N-DMBI display a low ionisation efficiency, i.e. the ratio of charges created per dopant molecule (cf. chapter 4 for details on ionisation efficiency), and suffer from gross phase-separation of unreacted dopant, which displays a low degree of miscibility with the host semiconductor.[103] As a result, for n-doped NDI-based polymers the electrical conductivity tends to be less than $\sim 0.1\,\mathrm{S\,cm^{-1}}$.[146]

This chapter will cover several approaches towards enhancing the compatibility and solubility of dopant/semiconductor systems. Firstly, I will investigate ternary blends of P3HT, F4TCNQ and several insulator polymer as an avenue to realize conducting bulk structures. Then, I will examine doping of conjugated polymers bearing polar side chains that are thought to enhance their compatibility with molecular dopants. A third concept that is covered is the addition of solubilizing (alkyl) chains to molecular dopants to increase their solubility.

3.1 Blending with Polar Insulating Polymers

Blending of polymers is an established method to combine different properties in one material. It is for example commonly used to adjust the mechanical and rheological properties. Blends comprising conjugated and commodity polymers are of interest for the realisation of cost-efficient bulk structures and can enhance device and material performance for e.g. OFETs,[102,147,148] organic solar cells[149,150] and organic thermoelectric generators.[151,152] A primary focus is often a good device performance at low semiconductor content, which is commonly achieved by cautiously chosen processing techniques. For example, careful crystallisation of the semiconductor before the semi-crystalline insulator polymer can result in superior device performance.[148,149] In case of amorphous matrix polymers controlled formation of nano-wires[152,153] or suppression of phase separation by rapid solvent removal can be used.[154] Commodity polymers with a moderate polarity are thought to provide improved compatibility with molecular dopants and the dopant:semiconductor

ion pair. I explored the use of the insulating polymers poly(ethylene oxide) (PEO) and poly(L-lactic acid) (PLLA) (figure 3.1) for ternary blends with P3HT and F4TCNQ (paper I). Both PLLA and PEO are relatively polar. PEO has previously been blended with P3HT, which aids the choice of processing schemes to control the nanostructure of blends.[155,156] Additionally, PEO and its shorter oligomers are known to have favourable interactions with ionic species[157] used for example as solid polyelectrolytes for Li-ion batteries.[158] The non-polar polymer PE is added to the analysis to test the importance of dipoles in the insulating polymers.

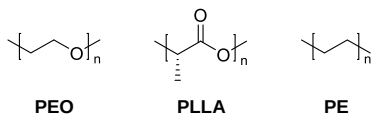

Figure 3.1: *Chemical structures of the insulating polymers poly(ethylene oxide) (PEO), poly(L-lactic acid) (PLLA) and polyethylene (PE).*

My initial work focused on finding a suitable processing scheme to realize ternary blends with PEO. Preparation of P3HT:PEO films drop-cast from ODCB:CB, followed by sequential doping with F4TCNQ in DCM as well as admixing of all three components and subsequent drop-casting at room temperature resulted in inhomogeneous films or strong vertical phase separation. Instead, solution co-processing at an elevated temperature of 110 °C allowed the preparation of visually homogeneous and several micrometer thick ternary blend films. Ternary blends with PLLA and PE were prepared in a similar fashion using a solution/casting temperature of 120 °C and the solvents ODCB and p-xylene, respectively.

The blend microstructures of F4TCNQ:P3HT at a molar ratio of 15 mol% with PEO, PLLA and PE were investigated by optical microscopy (figure 3.2). Optical micrographs of all blends reveal darker areas as a result of phase-separation. PLLA-blends display a coarse microstructure with large islands between 10 and 50 µm in size ascribed to

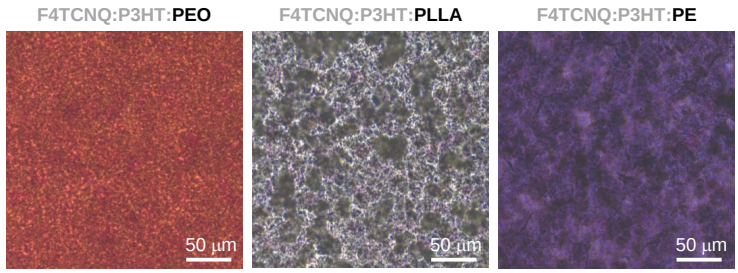

Figure 3.2: *Optical micrographs of drop-cast films of F4TCNQ:P3HT (*15 mol%*) with PEO (left), PLLA (middle) and PE (right); weight ratio of conjugated / insulator polymer is 1:9.*

F4TCNQ:P3HT and more transparent areas with PEO in between. Instead, blends with PEO feature a much finer microstructure with overlapping domains smaller than 10 µm, which is likely responsible for the higher electrical conductivity compared with PLLA (cf. figure 3.3). The different microstructures may be explained by the polarity of the matrix polymers. PEO should offer a good compromise in terms of compatibility with both P3HT and more polar F4TCNQ. In case of blends with PE intense vertical phase separation of F4TCNQ:P3HT aggregates is noted. This observation is explained with the non-polar character of PE prohibiting mixing with charged F4TCNQ:P3HT. Hence, I chose to focus the my analysis on blends with PEO.

I prepared films with different F4TCNQ molar fractions at a constant P3HT:PEO ratio of 1:9 and recorded their electrical conductivity (figure 3.3a). For details on electrical measurements of films refer to paper I. With increasing F4TCNQ fractions the electrical conductivity increases steadily up to a molar fraction of 20 mol%, where the conductivity levels off. A similar trend at an about one order of magnitude lower electrical conductivity is observed for P3HT:PLLA blends for the same range of compositions. The conductivity of neat F4TCNQ:P3HT is known to drastically decrease above 17 mol% due to excess doping in the conducting phase.[57] In case of the investigated ternary blends the conductivity remains nearly unchanged indicating that excess F4TCNQ is taken up by the insulator

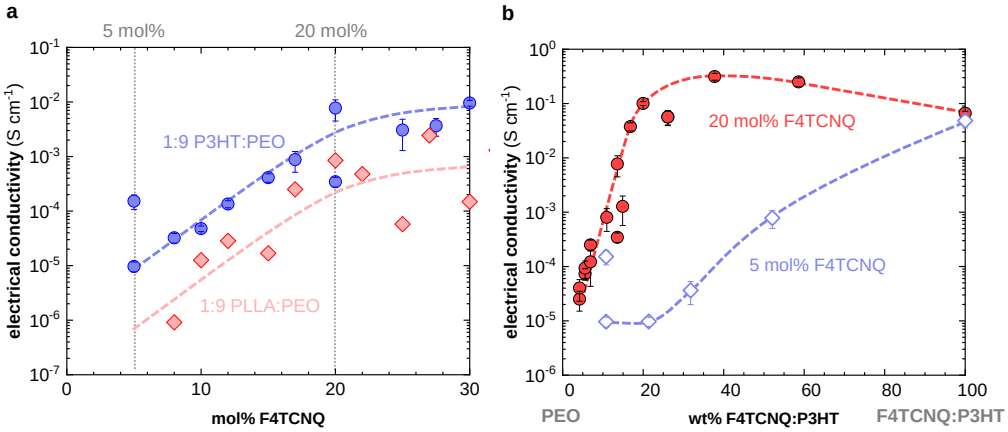

Figure 3.3: *Electrical conductivity of P3HT:PEO (1:9, blue) and P3HT:PLLA (1:9, red) at increasing F4TCNQ molar dopant fractions (a); electrical conductivity of F4TCNQ:P3HT:PEO blends with increasing F4TCNQ:P3HT fraction at 5 and 20 mol% (b). Dashed lines are a guide to the eye.*

phase instead. This is consistent with the observation that F4TCNQ can diffuse into PEO (paper I, SI figure 5).

To investigate the influence of the weight fraction of insulator polymer on the electrical properties, I cast films with different PEO fractions. The F4TCNQ molar fraction in these samples were kept constant at 5 mol% and 20 mol% relative to the P3HT content and are referred to as weakly and and strongly doped samples. Weakly and strongly doped samples display markedly different behaviours (figure 3.3b). A steady increase of the electrical conductivity of weakly doped blends by several orders of magnitude is observed with decreasing PEO content. Instead, for strongly doped blends the electrical conductivity raises sharply by about four orders of magnitude with increasing F4TCNQ:P3HT content below 20 wt% and reaches a maximum at about 40 wt%. The observed impact of the PEO content on the electrical conductivity can be explained with double percolation of F4TCNQ:P3HT rich domains in a PEO rich matrix that contains a fraction of more finely dispersed doped P3HT as indicated by current-sensing atomic force microcopy

undertaken by Andrés Gómez at ICMAB. Further, the addition of PEO slightly increased the ionisation efficiency for strongly doped blends.

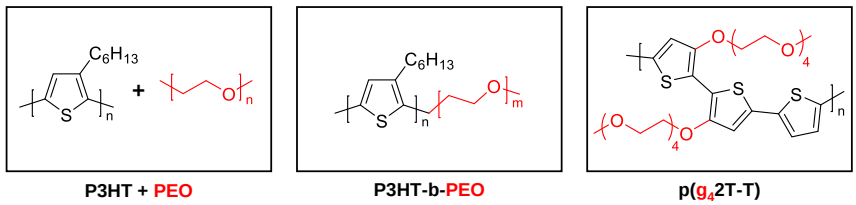

Figure 3.4: *Proposed ways to mitigate issues with the compatibility between conjugated polymers and dopant. Left: Blends of P3HT and PEO, Middle: Co-polymers with P3HT and PEO blocks, Right: Polythiophene with oligoethylene glycol side chains.*

Ternary blending of F4TCNQ:P3HT:PEO is deemed to not significantly enhance the processability of the doped conjugated polymer since processing still requires elevated temperatures. Further, undesired microscopically phase-separation occurs. However, the comparison between PEO, PLLA and PE implies a relatively high miscibility of PEO with F4TCNQ:P3HT, meaning that several other approaches employing polar polyethylene oxide/glycol structures may hold promise (figure 3.4). Uncontrolled phase separation may be overcome with block co-polymers, which offer control over microscopic phase separation by varying the length and interaction of the different blocks.[159] Co-polymers comprising P3HT and polar PEO blocks have been reported previously[160,161] and are expected to offer good miscibility with polar dopant molecules. Additionally, block co-polymers may be a tool to reduce the interfacial tension between the phases in P3HT:PEO blends for bulk structures.[162] Replacing the non-polar alkyl side chains in P3HT with polar ethylene glycol side chains is proposed as a second avenue to directly increase the polarity along the conjugated backbone. Polar side chains are expected to facilitate enhanced solubility of the polythiophene in polar organic solvents and aid the stability of the doped polymer against precipitation in the processing solvent. This approach will be covered in the following section.

3.2 Conjugated Polymers with Polar Side Chains

Although most soluble conjugated polymers bear non-polar aliphatic side chains, synthetic design of side chains offers a unique toolbox to tune their chemical and physical properties and enhance the performance of organic electronic devices.[163] For instance, polar side chains, such as oligoethylene glycol chains, promote the influx of ions for redox reactions inside of conjugated polymer films for, e.g. OECTs[164–166] and organic batteries,[167,168] due to favourable polar interactions. This type of side chain has also been suggested for chemical sensors,[169] and solar cells.[170] Since molecular doping entails the use of polar dopant molecules and the formation of charged species, I expect oligoethylene glycol side chains to greatly enhance molecular doping. In fact, Li *et al.* reported stronger interaction of both neutral and charged F4TCNQ with an oligoethylene glycol / sulfonic acid substituted polythiophene compared with P3HT, but only found a low electrical conductivity of $10^{-1}\,\mathrm{S\,cm^{-1}}$.[171]

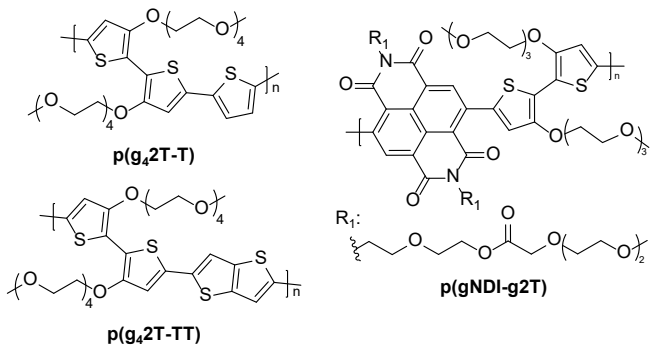

Figure 3.5: *Chemical structures of conjugated polymers with polar oligoethylene glycol side chains that I used in this thesis.*

A polythiophene, p($g_4$2T-T), and a polythienothiophene, p($g_4$2T-TT), with tetraethylene glycol side chains (figure 3.5), synthesised by Dominik Stegerer and Dr. Renee Kroon at Chalmers, were chosen as p-type polymers together with the dopant F4TCNQ. Despite a

tendency for p($g_4$2T-T) to aggregate, the polar side chain enabled processing from more polar solvents and solvent mixtures suitable also for F4TCNQ. Note that in order to allow fair comparison with P3HT the dopant molar fraction for doping of p($g_4$2T-T) is given per thiophene unit, i.e. $M_{\text{repeat unit}}/3$, whereas for all other polymers it is given relative to the polymer repeat unit. A markedly different appearance between doped P3HT and p($g_4$2T-T) was noted (figure 3.6). Doping of P3HT resulted in conspicuous precipitation in the form of black particles. Instead, F4TCNQ-doped p($g_4$2T-T) only exhibited slight coagulation, which could be mitigated by dilution, but appeared precipitate-free even after addition of as much as 10 mol% F4TCNQ. The formidable solution processability of p($g_4$2T-T) with F4TCNQ, which is ascribed to solvation of the doped polymer by polar side chains, allowed spin-coating of homogeneous thin films at room temperature.

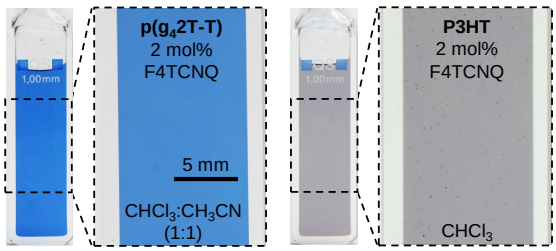

Figure 3.6: *Photographs of p($g_4$2T-T) (left) and P3HT (right) doped with 2 mol% F4TCNQ at a polymer concentration of* 0.2 g L^{-1}.

I used grazing-incidence wide-angle scattering (GIWAXS) to investigate the texture of ordered domains in p($g_4$2T-T) doped with F4TCNQ as well as neat F4TCNQ embedded in an amorphous polystyrene (PS) matrix (figure 3.7). For neat F4TCNQ a single scattering peak at $\sim$7.7 nm^{-1} is noted, which has also been observed for high F4TCNQ loadings in P3HT[57]. In case of p($g_4$2T-T) a scattering peak at this position is not present even for high dopant concentrations of 20 mol%. This suggests that excess dopant is molecularly dispersed in the polymer film, which I assign to the favourable interactions with the polar side chains.

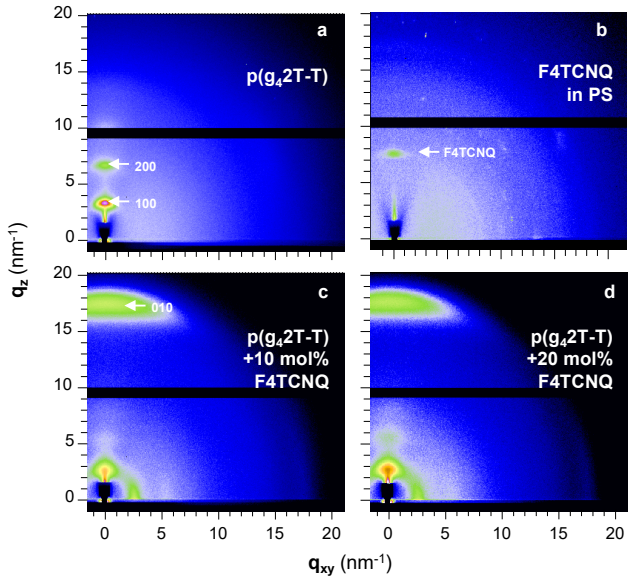

Figure 3.7: *GIWAXS detector images recorded at Cornell High Energy Synchroton Source (CHESS) for thin films of neat p($g_4$2T-T) (a), F4TCNQ embedded in an amorphous PS matrix (b), p($g_4$2T-T) doped with 10 (c) and 20 mol% (d).*

A further indication for the solubilizing effect of the side chains is a stable electrical conductivity above a molar fraction of 10 mol%, where the maximum electrical conductivity of up to 100 S cm^{-1} is reached (cf. figure 3.10). I hypothesise that excess dopant forms relatively finely dispersed aggregates with minimal impact on the polymer nanostructure. Instead, for co-processed F4TCNQ:P3HT films, which also require a higher dopant molar fraction of at least 17 mol% to reach a significantly lower maximum conductivity, a sharp drop of the conductivity due to dopant aggregates that interrupt the semiconductor nanostructure is observed.[57]

To test if polar side chains can also aid n-doping, a polymer featuring the identical conjugated backbone as p(NDI2OD-T2), but with oligoethylene glycol-based side chains on both the NDI acceptor and the bithiophene donor was selected (figure 3.5) and doped with N-DMBI. The dopant is known for its tendency to aggregate when used

in combination with e.g. PCBM[172] and p(NDI2OD-T2).[103] Atomic force microcopy undertaken by Dr. Anna Hofmann at Chalmers was employed to compare the surface morphology of thin films (figure 3.8) and revealed that dopant aggregation is largely suppressed up to a dopant molar fraction of 20 mol%. Instead, Schlitz *et al.* report the appearance of a significant concentration of aggregates at already 9 mol% dopant in p(NDI2OD-T2). The improved miscibility is also supported by another independent report of a similar NDI-based co-polymer doped with the same dopant.[173]

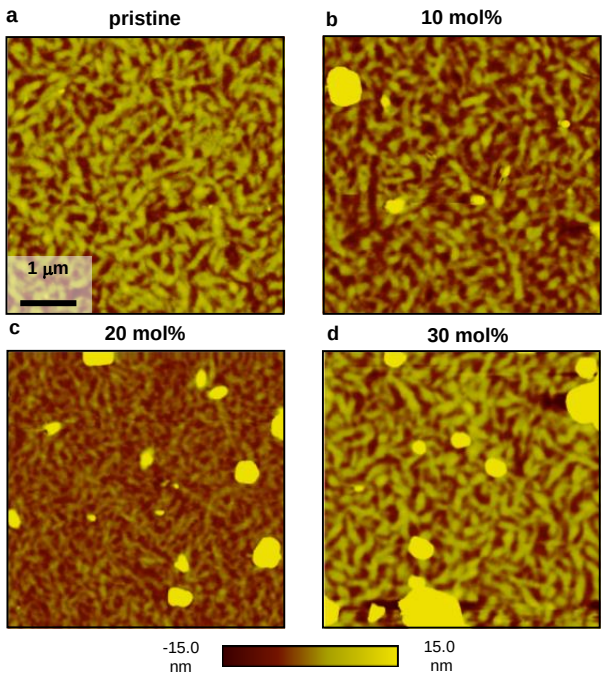

Figure 3.8: *AFM height images of pristine p(gNDI-gT2) (a) and doped with 10 (b), 20 (c) and 30 mol% N-DMBI (d).*

Furthermore, a high charge carrier density of $\sim 10^{19}$ cm^{-3} was estimated by both modelling of the temperature-dependent conductivity by Prof. L.J. Anton Koster's group at the University of Groningen and quantitative electron paramagnetic resonance (EPR) spectroscopy by Dr. Till Biskup at Freiburg University (paper II, figure 3). Previous reports

of p(NDI2OD-T2) deduced a very low ionisation efficiency of only ∼1 %, whereas for p(gNDI-gT2) doped with 20 mol% N-DMBI an at least ten times higher doping efficiency of ∼13 % can be obtained. Since doping with N-DMBI is thought to entail the transfer of a hydride instead of simple charge transfer,[108] it is unlikely that the higher doping efficiency is a result of the slightly different EAs of the two polymers, i.e. 4.1 eV for p(gND-gT2)[166] and 4.0 eV for p(NDI2OD-T2).[174] Instead, increased ionisation efficiency is assumed to be a result of the better miscibility of dopant and conjugated polymer. Similarly, an enhanced ionisation efficiency of a PCBM derivative carrying an oligoethylene glycol side chain doped with N-DMBI has been reported by Liu *et al.*, which compared with PCBM reached a more than two orders of magnitude higher electrical conductivity of $2\,\mathrm{S\,cm^{-1}}$.[175,176]

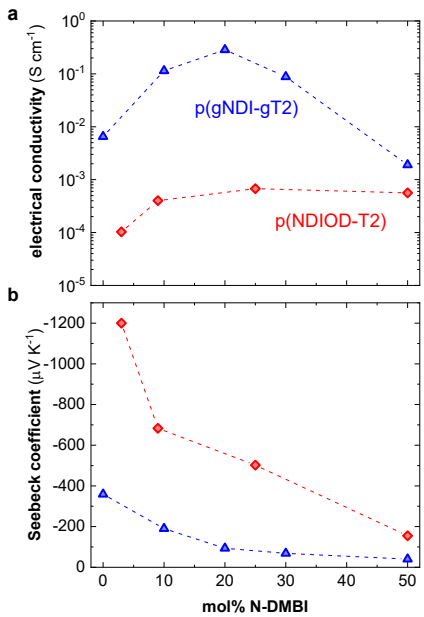

Figure 3.9: *Electrical conductivity (a) and Seebeck coefficient (b) of p(gNDI-gT2) (blue) and p(NDI2OD-T2) doped with various concentrations of N-DMBI. Electrical properties were undertaken by Dr. Hengda Sun, Linköping University, and myself.*

The high charge carrier concentration is further corroborated by measurements of the Seebeck coefficient and the electrical conductivity of thin spin-coated films. (figure 3.9). For dopant molar fractions between 20 and 30 mol% p(gNDI-gT2) exhibits a three to five times lower Seebeck coefficient compared with p(NDI2OD-T2) as a consequence of the higher charge carrier density. Further, a significantly higher maximum electrical conductivity of $0.3\,\mathrm{S\,cm^{-1}}$ is obtained for doping with 20 mol% N-DMBI, whereas for doping of p(NDI2OD-T2) the conductivity remains below $10^{-3}\,\mathrm{S\,cm^{-1}}$ for all dopant molar fractions. Addition of more N-DMBI to p(gNDI-gT2) leads to a rapid decrease of the electrical conductivity, which can be explained by interruption of the nanostructure as indicated by excess dopant domains on top of the films.

I argue that polar side chains are a universal tool to enhance p- and n-doping of conjugated polymers since they improve the compatibility with molecular dopants. Different conjugated backbone designs, such as DPP-based conjugated polymers that exhibit higher charge carrier mobilities,[177] in combination with polar side chains may lead to further improved the electrical conductivities. The dopant:semiconductor interactions could be further influenced by other polar structures, such as amine, alcohol or ester functionalities. However, these functionalities could suffer from strong interactions with dopants or the polymer backbone.

3.3 Dopant Molecules with Side Chains

Another logical approach to enhance doping of conjugated polymers is to adjust the chemical structure of the molecular dopant instead of the conjugated polymer. Much synthetic effort has been dedicated to adjusting the energy levels or mechanism of dopants,[67,104,112,145,178–180] but surprisingly only few studies focus on increasing the solubility of molecular dopants. For example Qui *et al.* modified the n-dopant N-DMBI by the addition of an oligoethylene glycol side chain in order to increase the miscibility of the dopant with a PCBM derivative that bears the same side chain. This allowed to half the required doping fraction from 40 to 20 mol% while reaching a maximum electrical conductivity of almost $2\,\mathrm{S\,cm^{-1}}$.[181] The p-dopant F4TCNQ has been used as a parent molecule by sacrificing either one or more fluorine[179] or cyano groups[52] to add different functionalities that are thought to improve dopant processability. Li *et al.* showed that the solubility in chloroform was significantly increased by replacement of one cyano group with a methyl ester or an octyl ester, which only resulted in a slight reduction of the EA (0.1 – 0.2 eV) of the dopants compared with F4TCNQ. In doping experiments with P3HT the two mono-substituted dopants, F4MCTCNQ and F4OCTCNQ (figure 3.10; top), showed a promising high electrical conductivity at lower dopant molar fractions, which was attributed to a higher ionisation efficiency.[52] Furthermore, F4MCTCNQ proved to have a much lower diffusion coefficient compared with F4TCNQ, which was used for microscopic patterning by a doping-induced solubility control mechanism.[73,182]

I measured the electrical conductivity of thin spin-coated films of p($g_4$2T-T) co-processed with F4MCTCNQ and F4OCTCNQ (supplied by Prof. Mark Mascal, University of California, Davis) from a 1:1 mixture of chloroform/acetonirile and compared them with films doped with F4TCNQ (figure 3.10; bottom). Doping with both dopants results in an electrical conductivity between 5 and $9\,\mathrm{S\,cm^{-1}}$ at 10 mol%, which for F4MCTCNQ increases to 60 to $70\,\mathrm{S\,cm^{-1}}$ for molar dopant fractions of 15 and 20 mol%. Instead,

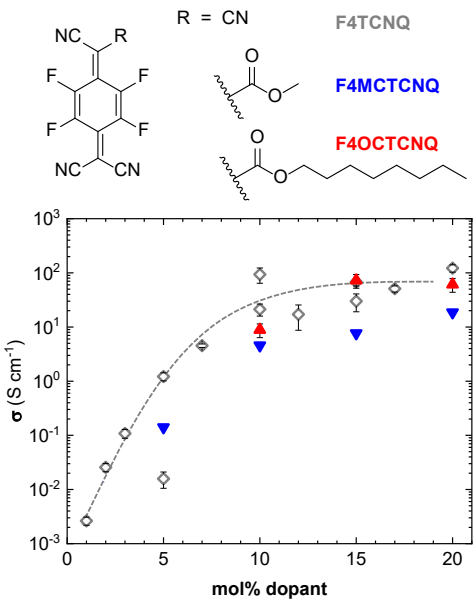

Figure 3.10: *Chemical structures of dopants (top) and electrical conductivity of p($g_4$2T-T) doped with F4TCNQ, F4MCTCNQ and F4OCTCNQ (bottom).*

F4MCTCNQ doped films feature a lower electrical conductivity of up to 20 S cm^{-1} for similar molar fractions. Hence, doping with F4OCTCNQ can reach comparably high electrical conductivities like F4TCNQ in p($g_4$2T-T), whereas doping with F4MCTCNQ leads to a slightly lower electrical performance. The effect of the higher solubility of dopants in chloroform, probably accountable for more efficient doping of P3HT,[52] is likely to be less important in case of p($g_4$2T-T) since the used solvent mixture ($CHCl_3$:CH_3CN, 1:1) also allows dissolution of F4TCNQ at high concentrations. The higher conductivity reached when doped with F4OCTCNQ compared with F4MCTCNQ suggests that its longer aliphatic chain does not affect the miscibility with the polar polythiophene. A more adapted system could be developed by replacing the alkyl side chains with oligoethylene glycol chain, thereby matching the polarity of both components, as shown for n-type doping of PCBM.[181]

4 Energetics of Molecular Doping

As introduced in chapter 2 organic semiconductors undergo charge transfer with redox dopants, such as F4TCNQ. The extent of this charge transfer depends on a variety of factors, which are material- and nano-/microstructure-dependent. Currently there is no universal picture that can explain in which cases partial or complete charge transfer occurs.[37] Partial charge transfer is unfavoured since it requires thermal ionisation of the charge transfer complex to form charge carriers.[38] Instead, complete charge transfer directly leads to the formation of ion pairs that can dissociate to form free charge carriers, i.e. cations in the case of p-doping (cf. section 4.1.2).[183] FTIR is a powerful tool to probe the extent of charge transfer for doping reactions that involve F4TCNQ. The shift of the cyano (CN) stretch vibrations compared with the neutral dopant indicates the degree of charge transfer.[61]

One important factor is the difference between the IE and EA of the donor and acceptor and it is often stated that for the formation of an ion pair the IE of the donor must be less than the EA of the acceptor (IE < EA). In some cases, however, complete charge transfer was observed even though the EA of the acceptor was below the IE of the donor.[52,65,184] Experimental values of IE and EA only provide a limited description since the local IE/EA can be very different due to the close proximity of the ionized dopant and semiconductor. A more complete relation between the extent of charge transfer (δ), the EA and IE as well as the electrostatic (Coulomb) interactions can be taken from the field of charge-transfer salts, where the energy difference between IE and EA is amended with the Madelung energy:[46]

$$E(\delta) = (IE - EA)\delta - k_e \frac{q^2}{r}\delta^2 \tag{4.1}$$

where q is the elementary charge, r the distance between hole and electron k_e the Coulomb constant, which is defined as $k_e = 1/4\pi\varepsilon_0$.[37,185] To account for the specific dielectric

environment the vacuum dielectric constant ε_0 should replaced with the absolute dielectric constant for a certain material ε (cf. section 4.2).

The relation in equation 4.1 suggests that ion pair formation, i.e. $\delta = 1$, is favoured for a large offset between IE an EA (IE << EA), which could be achieved by lowering the IE of the donor or increasing the EA of the acceptor. For example, in case of p-doping, stronger dopants (compared with F4TCNQ) have been used to dope polymers that feature a higher IE, such as DPP-based polymers,[67,186] but are limited due to their high reactivity leading to a low stability. The IE of conjugated polymers can be lowered through increasing their electron density by substitution with electron donating moieties. This is the case for both p($g_4$2T-T) and p($g_4$2T-TT), which feature an oxygen atom directly attached to their backbone resulting in decreased IEs of ∼4.6 and ∼4.5 eV compared with their analogues P3HT (∼5.0 eV) and pBTTT (∼5.2 eV). In the following section the impact of this lower IE on molecular doping with F4TCNQ and DDQ will be described, followed by a discussion on the above-mentioned effects of electrostatic interactions and the influence of the dielectric environment.

4.1 Energy Level Offset

4.1.1 Weaker Dopants

The prototypical p-type conjugated polymer regio-regular P3HT is readily doped by F4TCNQ as discussed previously. The suitable offset between the IE of P3HT and the EA of F4TCNQ typically facilitates integer electron transfer from P3HT to F4TCNQ,[61] with the exception of one recently reported polymorph that only undergoes partial charge transfer (cf. section 2.1.1).[68] Doping of P3HT with weaker electron acceptors such as DDQ[187,188] is disfavoured.[70,189,190] This is because of its lower EA of ∼4.6 eV[70,191]

compared with F4TCNQ, which presents a significant mismatch with the IE of P3HT (figure 4.1).

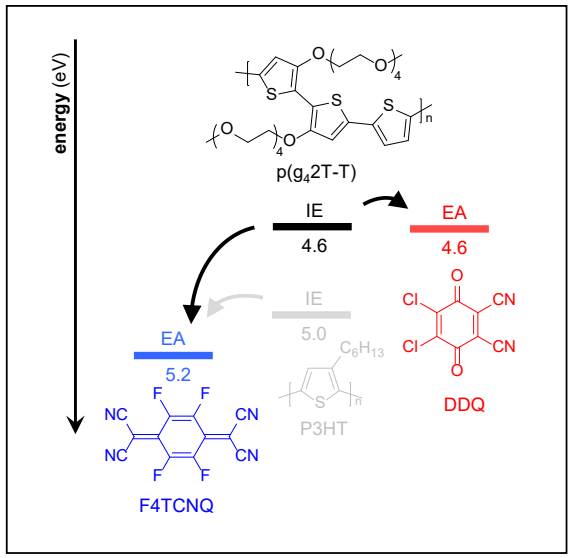

Figure 4.1: *The decreased ionization energy of p(g$_4$2T-T) compared with P3HT allows effective doping with significantly weaker dopants, such as DDQ.*

I investigated doping of p(g$_4$2T-T) with DDQ by measuring the electrical conductivity and optical spectra of thin spin-coated films (figure 4.2). Co-processed films exhibit an electrical conductivity of $\sim$0.1 S cm^{-1} for a dopant molar fraction of 5 mol%, together with reduced optical absorption of the polymer around 2.0 eV and the appearance of polaronic features below 1.4 eV. Upon further doping the conductivity increases by about three orders of magnitude to a high maximum value of 50 S cm^{-1} at 15 mol%. Interestingly, features in the optical spectra of the DDQ-doped polymer for 10 and 15 mol% between 2.0 and 2.5 eV (grey circle) match the reported spectra of the DDQ anion [192] and may suggest full charge transfer. However, they overlap with the absorption of the neutral polymer and the absorption intensity above 2.5 eV increases simultaneously, which could indicate both neutral and anionic DDQ. Therefore, a conclusive interpretation of the charge transfer characteristics between p(g$_4$2T-T) and DDQ based on UV-vis absorption

is not possible. Nevertheless, electrical conductivities are comparable to doping with F4TCNQ and demonstrate the high degree of doping with the weaker dopant DDQ. This is explained by the low IE of p($g_4$2T-T), which should favour ion pair formation with DDQ. Note, that full and partial charge transfer may coexist, similar to reports for P3HT and F4TCNQ.[193]

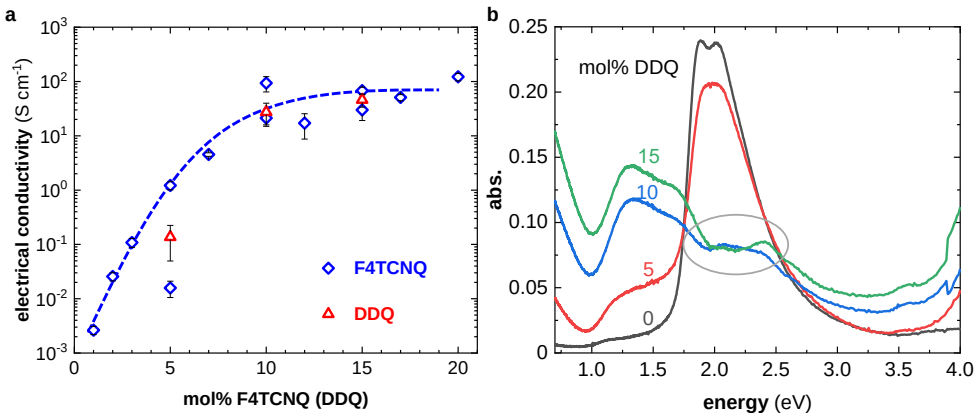

Figure 4.2: *Electrical conductivity of p($g_4$2T-T) doped with F4TCNQ (blue) and DDQ (red) (a); thin film optical absorption spectra of neat p($g_4$2T-T) and doped with* 5, 10 *and* 15 mol% *DDQ. Dashed line is a guide to the eye.*

4.1.2 Double Doping

Charge carriers created by ion pair formation (or thermal ionisation of a charge transfer complex) must dissociate in order to contribute to conductivity (here exemplified for p-doping):[194]

$$\mathrm{D} + \overline{\mathrm{D}}\mathrm{A} \quad \overset{\text{(i)}}{\rightleftharpoons} \quad \mathrm{D} + \left[\overline{\mathrm{D}}^{+\delta}\mathrm{A}^{-\delta}\right] \quad \overset{\text{(ii)}}{\rightleftharpoons} \quad \mathrm{D}^{+} + \overline{\mathrm{D}}\mathrm{A}^{-} \tag{4.2}$$

During the ionisation step (i) an electron is transferred from a donor molecule $\overline{\mathrm{D}}$ (the macron indicates vicinity to the acceptor) to an acceptor molecule A. The result is a charge

transfer complex $\left[\overline{D}^{+\delta}A^{-\delta}\right]$ where $0 \leq \delta \leq 1$ denotes the degree of charge transfer. In case of full charge transfer a cation $\overline{D}^{+}$ and an anion A^{-} form and remain coulombically bound to each other. During the second step (ii) dissociation of the charge transfer complex leads to a cation D^{+} located at a site that is sufficiently far away from the anion to minimize any Coulomb interaction with the 'parent' donor. Note that especially at high dopant concentrations this site may be close to one or more anions. The final state (D^{+}) is to be thought of as a hole charge carrier that participates in transport. Both steps are reversible and at equilibrium the ionisation efficiency is given by $\eta_{\text{ion}} = \Sigma_{\delta=1}\delta N_{A^{-\delta}}/N_A \times 100\%$, where $N_{A^{-\delta}}$ is the number of anions with charge $-\delta$ and N_A is the total number of acceptor molecules. At low doping concentrations, where a hole can escape the Coulomb capture radius of its parent donor without being captured by another ion, leading to the formation of a free charge carrier, a dissociation efficiency $\eta_{\text{diss}} = {}^{N_{D^+}}/_{N_A} \times 100\%$ can be defined, where N_{D^+} is the number of hole charge carriers. However, in the view of the fundamental equivalence of dopant molecules at high dopant concentrations > 1 mol% it is problematic to define a dissociation efficiency since there are no sites that are not within the Coulomb capture radius of, or even adjacent to, an ion.[195,196] The term doping efficiency, which is often found in the literature, is not clearly defined in this context and has been used to describe both the ionisation and dissociation efficiency.

Low ionisation efficiencies, far below the current theoretical limit of one charge per dopant, i.e. $\eta_{\text{ion}} < 100\,\%$, require the addition of large amounts of dopants to achieve the desired electrical conductivity. In turn, this has detrimental consequences for the nanostructure of the semiconductor further limiting the electronic performance. One powerful avenue to avoid these complications would be to achieve the transfer of more than one charge per dopant molecule. In fact, the molecular dopant F4TCNQ can function as a two electron acceptor, by the formation of dianions in charge-transfer salts[197–199] and through photogeneration in single crystals.[200,201] However, presently doping of conjugated polymers with F4TCNQ only focuses on the transfer of a single electron to form F4TCNQ

anions. A double charge transfer from F4TCNQ to a conjugated polymer and hence the formation of dianions should give rise to a maximum achievable ionisation efficiency of $\eta_{\text{ion}} = 200\,\%$ and a significant reduction of the necessary dopant fraction.

In paper IV we report the formation of F4TCNQ dianions in the conjugated polymer p($g_4$2T-TT). Double doping is shown to be facilitated because of the low IE of p($g_4$2T-TT), significantly below the EA^0 ~5.2 eV of neutral F4TCNQ as well as the EA^- ~4.7 eV of the F4TCNQ anion (figure 4.3).

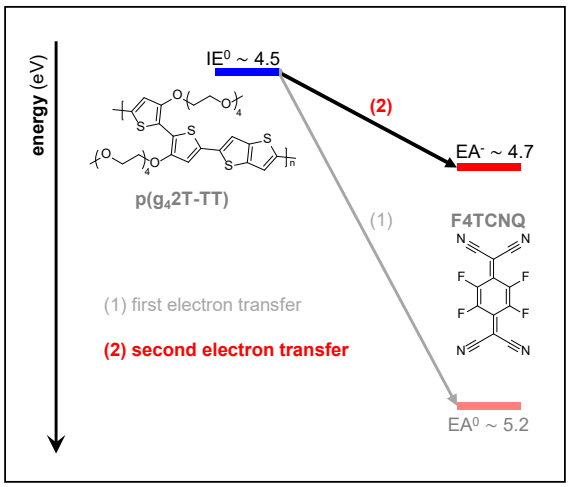

Figure 4.3: *A single F4TCNQ molecule can accept two electrons from conjugated polymers if the offset between IE of the polymer is similar to the EA^- of the dopant anion. Energy levels IE and $EA^{0/-}$ were determined by cyclic voltammetry undertaken by Dr. Anna Hofmann at Chalmers.*

To allow qualitative and quantitative analysis of present F4TCNQ species the mono- and di-litium salts of F4TCNQ ($Li^+F4TCNQ^{\bullet-}$ and $2Li^+F4TCNQ^{2-}$) were synthesised by Dr. Renee Kroon at Chalmers according to an adapted literature procedure.[197] These, as well as neutral F4TCNQ, were dissolved in acetonitrile and UV-vis and FTIR spectra were recorded (figure 4.4 and paper IV, SI figure 3). The spectra can be used to estimate the number of neat, anionic and dianionic F4TCNQ (cf. paper IV).

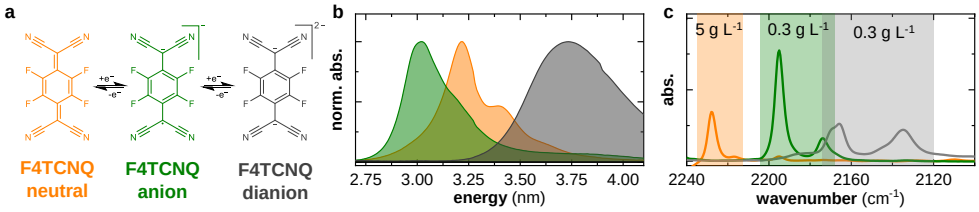

Figure 4.4: *Chemical structures (a), UV-vis spectra (b) and FTIR spectra of CN-vibration (c) of neutral, anionic and dianionic F4TCNQ.*

UV-vis absorption spectra and FTIR absorption of the CN-stretch vibration confirm the formation of F4TCNQ dianions in p($g_4$2T-TT) (paper IV, figure 1). The number of F4TCNQ molecules in solution and films that have reacted with p($g_4$2T-TT) to become anions and dianions was estimated by least-square fitting of the UV-vis absorption spectra between 2.5 and 4.0 eV (figure 4.5). In this region the spectra were deconvoluted with the absorption coefficients of neutral, anionic and dianionic F4TCNQ as well as a Gaussian centered at 2.4 eV and a 'baseline' (the two latter are thought to represent contributions from the amorphous polymer). Fits of spectra taken of liquid samples achieve the best description of the experimental data, whereas broadening of the spectral features and peak shifts in solid film samples complicate fitting, which results in somewhat lower conformity of the fits and experimental data.

The fractions of neat, anionic and dianionic F4TCNQ in p($g_4$2T-TT) strongly depend on the absolute number of F4TCNQ molecules in the conjugated polymer (figure 4.7). For a molar fraction of 10 mol% F4TCNQ and below all F4TCNQ molecules undergo charge transfer with p($g_4$2T-TT) with more than 90 % being present as dianions resulting in a high ionisation efficiency η_{ion} of over 190 %. FTIR spectra were used to confirm the relative amounts of F4TCNQ anions and dianions (cf. paper IV, figure 3). The nearly unchanged absolute F4TCNQ dianion concentration from 10 to 40 mol% F4TCNQ is explained with the relatively high polaron density of one charge per approximately five polymer repeat units at 10 mol%. The lack of sufficiently undoped regions in the polymer

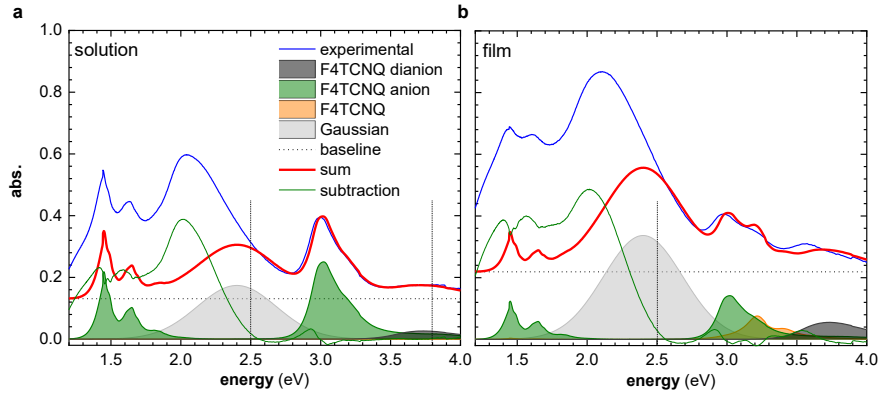

Figure 4.5: *Least square fits to the solution (a) and film (b) absorption spectra of p($g_4$2T-TT) doped with 10 mol% F4TCNQ using the extinction coefficients of F4TCNQ, its anion and dianion and a Gaussian in the region, where the polymer absorbs.*

is thought to allow formation of additional anions leading to an increased polaron density until 30 mol%, but to prohibit further dianion formation.

In paper II a similar fitting procedure was used to estimate the concentrations of neat F4TCNQ and its anions in p($g_4$2T-T) (paper II, figure 3), but neglected dianions since their presence was not anticipated at the time this paper was written. However, UV-vis and FTIR spectra (paper II, figure 2 and 3) indicate F4TCNQ dianions and, hence, the data was revisited and fitted according to the procedure above (figure 4.6). For molar dopant fractions of 5 mol% (per repeat unit) and below a high concentrations of dianions between 60 and 80 % is estimated. Higher dopant fractions are associated with a strong decrease of the dianion concentration below 10 % (cf. ionisation efficiency, figure 4.8). Note that, paper II already mentions the low fit accuracy for samples with $\leq$5 mol% dopant. Nevertheless, previous analysis qualitatively agrees with the new interpretation for higher dopant fractions.

Interestingly, the ionisation efficiency found for p($g_4$2T-TT) doped with F4TCNQ is consistently higher than for p($g_4$2T-T) and drops for a much lower F4TCNQ molar fraction.

The higher tendency of p($g_4$2T-TT) to form F4TCNQ dianions/anions is tentatively ascribed to the slightly lower IE of ∼4.5 eV compared with p($g_4$2T-T) (∼4.6 eV). However, other possible reasons may include structural effects as indicated by different GIWAXS textures of the doped polymers (cf. figure 3.7 and paper IV, SI figure 15) and increased charge delocalisation in p($g_4$2T-TT) due to higher backbone planarity in analogy with P3HT/pBTTT.[29,202]

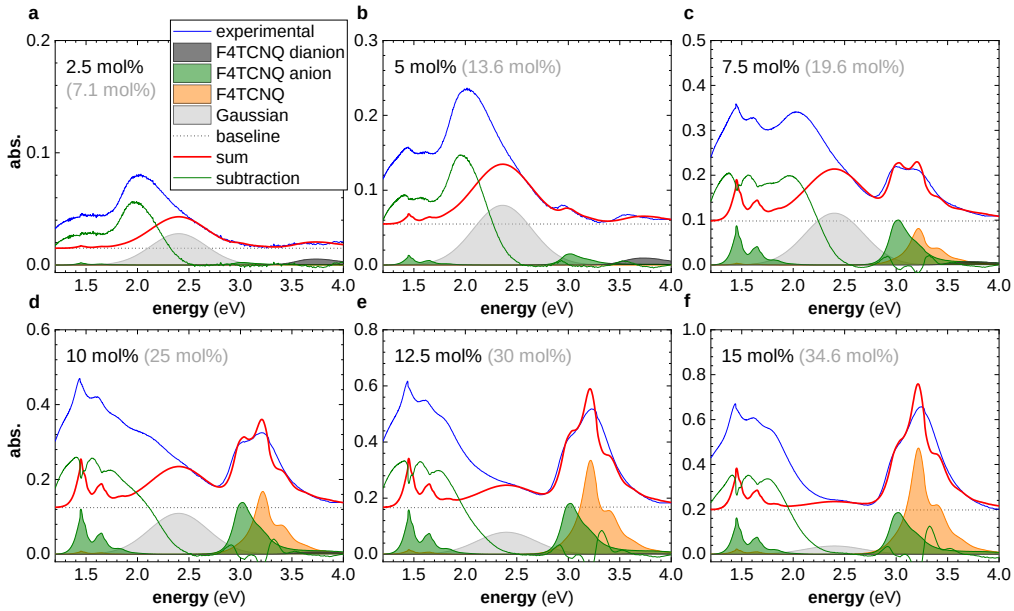

Figure 4.6: *Least square fits to the film absorption spectra of p($g_4$2T-T) doped with F4TCNQ at dopant molar fractions per thiophene ranging from* 2.5 *to* 15 mol%. *F4TCNQ molar fractions in brackets are calculated versus the polymer repeat unit.*

To further probe F4TCNQ dianion formation p($g_4$2T-TT) was doped directly with $Li^+F4TCNQ^{\bullet-}$. FTIR intensities of the CN vibrations of anions and dianions were used to determine their concentrations in thin films and estimate the ionisation efficiency (figure 4.8a). Near complete formation of F4TCNQ dianions can be observed for $\eta_{ion} \sim 10$ mol% followed by a gradual decrease of the anion to dianion ratio. Since $Li^+F4TCNQ^{\bullet-}$ can only accept one further electron a maximum ionisation efficiency of ∼100 % is observed, whereas

doping with F4TCNQ gives rise to double as many charges. As a result, significantly different electrical properties are observed for doping with F4TCNQ and $Li^+F4TCNQ^{\bullet-}$. Doping with F4TCNQ results in an electrical conductivity of $2\,S\,cm^{-1}$ at only 10 mol%, which increases to a maximum conductivity of $\sim 100\,S\,cm^{-1}$ for 40 mol%. For a dopant molar fraction of 50 mol% F4TCNQ the electrical conductivity drops, which is ascribed to the high dopant content that is likely to interrupt the nanostructure. Instead, p($g_4$2T-TT) doped with $Li^+F4TCNQ^{\bullet-}$ exhibits a consistently lower electrical conductivity of $1\,S\,cm^{-1}$ at 10 mol% that increases to $18\,S\,cm^{-1}$ for 40 mol%.

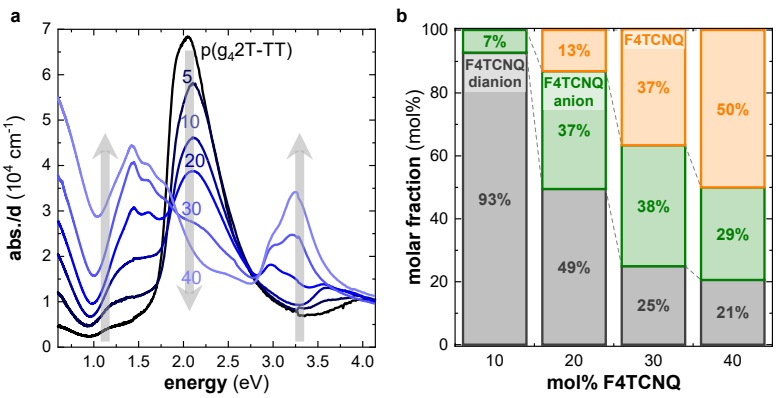

Figure 4.7: *UV-vis absorption spectra of p($g_4$2T-TT) (a) and molar fraction of neutral, anionic and dianionic F4TCNQ formed after doping with different amounts of F4TCNQ.*

Doping of p($g_4$2T-TT) with F4TCNQ results in notably higher Seebeck coefficients compared with $Li^+F4TCNQ^{\bullet-}$. For both dopants GIWAXS measurement indicate similar changes to the semiconductor nanostructure, which are excluded as a cause for the significantly different electrical properties. Therefore, the Seebeck coefficients allow direct comparison of the number of mobile charge carriers in samples doped with F4TCNQ and $Li^+F4TCNQ^{\bullet-}$ (paper IV, SI). Indeed, twice the amount of mobile charge carriers is found for doping with 10 mol% F4TCNQ compared with $Li^+F4TCNQ^{\bullet-}$ as a result of double charge transfer from F4TCNQ to p($g_4$2T-TT).

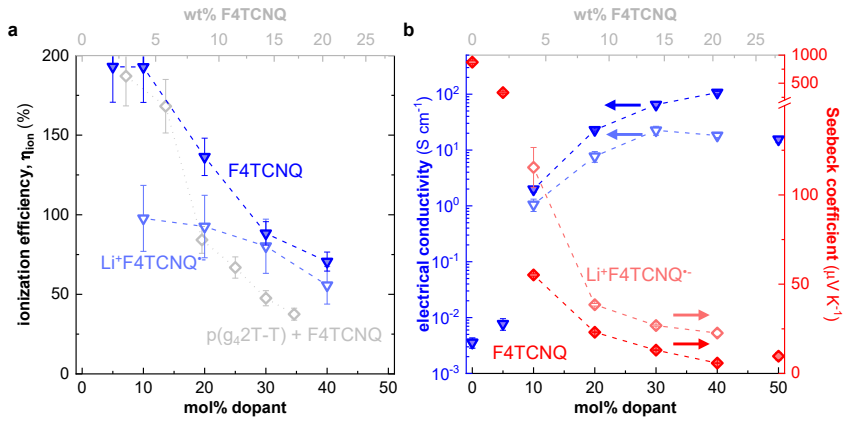

Figure 4.8: *Ionization efficiency* η_{ion} *(a), electrical conductivity and Seebeck coefficient (b) of p(*g_4*2T-TT) doped with F4TCNQ and Li*$^+$*F4TCNQ*$^{\bullet-}$*. Grey data in (a) is the revised ionization efficiency for p(*g_4*2T-T) doped with F4TCNQ (paper II); here dopant molar fraction is given relative to the polymer repeat unit.*

The high charge carrier density in p($g_4$2T-TT) doped with F4TCNQ was further corroborated by ultraviolet photoelectron spectroscopy (UPS) conducted by Dr. Anna Hofmann and Dr. Xianjie Liu at Linköping University (paper IV, figure 5). Additionally, for low dopant fractions (0.5 mol%) a significantly higher dissociation efficiency of ~172 % was extracted from Mott-Schottky diodes for doping with F4TCNQ compared with ~76 mol% for Li$^+$F4TCNQ$^{\bullet-}$. These measurements were undertaken by Dr. Hengda Sun at Linköping University, Campus Linköping. Furthermore, kinetic Monte Carlo simulations by Prof. Martijn Kemerink revealed a higher number of charges that significantly contribute to conductivity at a given point in time for doping with F4TCNQ.

The influence of the IE of the conjugated polymer on the formation of dopant dianions was further explored by doping of p($g_4$2T-TT) with the weaker and stronger dopants F2TCNQ and F6TCNNQ. Despite an EA$^-$ ~4.5 eV of F2TCNQ, which is similar to the IE of the polymer, only anions were observed in FTIR spectra (paper IV, SI figure 7). Instead, doping with F6TCNNQ featuring an EA$^-$ ~4.8 eV gave rise to dianions since EA$^-$ << IE.

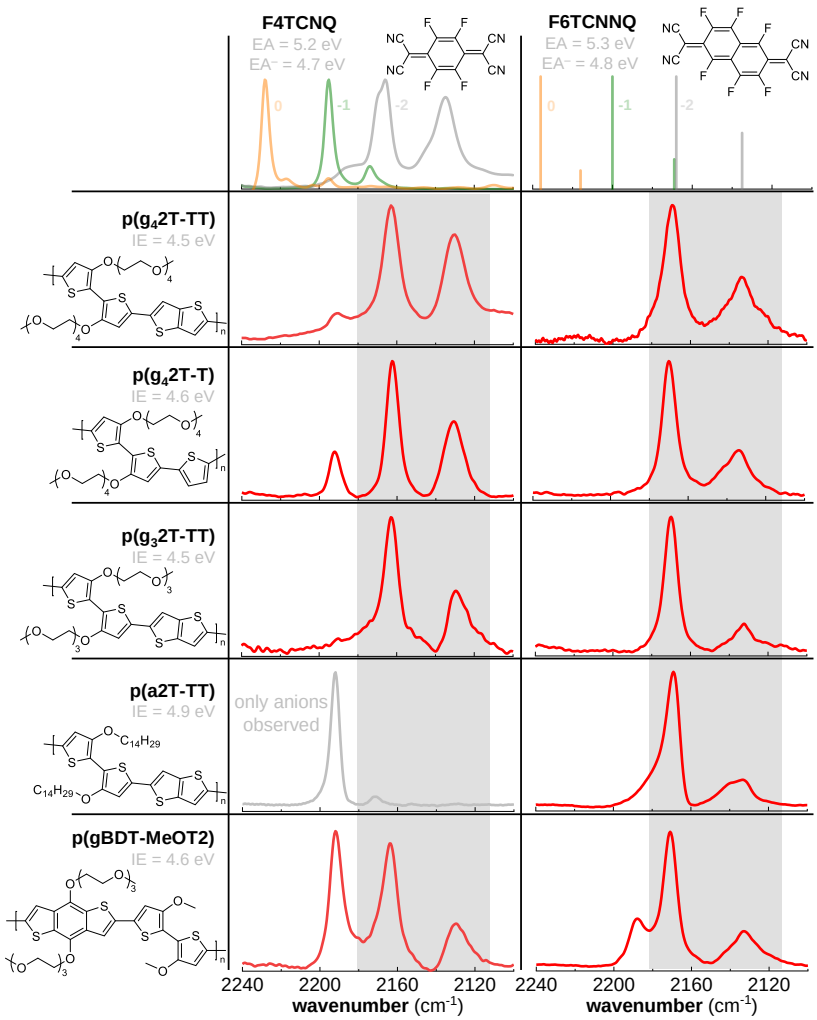

Figure 4.9: *Summary of conjugated polymer / dopant pairs with confirmed double doping; FTIR absorption spectra of the CN stretch-vibrations of polymers doped with F4TCNQ and F6TCNNQ in the range between 2240 and 2100* cm^{-1}*. Spectra are normalized to their highest intensity and y-axis was removed for clarity. Intensities of neat, anionic and dianionic F6TCNNQ are taken from DFT predictions in reference* ***203****.*

On the contrary, for doping of pBTTT, which features an IE of ∼5.2 eV, with F6TCNNQ only anions were observed (paper IV, figure 2). Several other dopant/conjugated polymer combinations leading to dopant dianion formation are summarized in figure 4.9. All listed polymers feature an IE that is below 5 eV and, with the exception of p(a2T-TT), also below the EA^- of F4TCNQ and F6TCNNQ. The low IE of the conjugated polymers is thought to aid dianion formation providing a sufficient energetic offset to allow the transfer of a second charge from the conjugated polymer to the dopant anion. However, for p(a2T-TT) the formation of F6TCNNQ dianions was observed despite $EA^- < IE$, which is explained with an influence of the electrostatic interactions between dopant and semiconductor covered in section 4.2.

Finally, I investigated whether the molecular weight of the polymer and the side chain length influences double doping (see paper IV, SI for experimental information). For thin films of three fractions of p($g_4$2T-TT) with different molecular weight significantly different ratios of F4TCNQ anions to dianions were found, which indicates that double doping may be further influenced by the molecular weight of the polymer. Additionally, for p($g_3$2T-TT) (see figure 4.9 for structure), which features shorter oligoethylene glycol side chain, a higher dianion to anion ratio was found. Preliminary result indicate a stronger tendency to aggregate of the polymer with a shorter oligoethylene glycol side chains, which may influence double doping. Further studies are necessary to understand the effect of polymer structure and film nanostructure on double doping.

I argue that double doping is a generic principle, which may apply to a wide range of organic semiconductors with adequate energy levels, and therefore may allow to significantly reduce the required dopant volume/weight fraction. For doping of p($g_4$2T-TT) with 10 to 40 mol% F4TCNQ a lower-bound charge carrier mobility range $\mu \sim 0.06$ - $2\,cm^2\,V^{-1}\,s^{-1}$ was deduced by counting all anions and dianions. Thus, application of double doping for conjugated polymers featuring higher mobilities may allow to significantly increase the electrical conductivity at low dopant loadings.

4.2 Electrostatics & Dielectric Environment

Electrostatic interactions between donor and acceptor are a second important factor that can influence the extent of charge transfer, and, in addition, are also critical for the delocalisation and transport of charges. In case of the former, favourable electrostatic interactions in a donor:acceptor pair may override an eventual mismatch of the energy levels, i.e. EA < IE, to complete full charge transfer. For instance, Mityashin *et al.* found that pentacene:F4TCNQ undergo full charge transfer as a result of favourable electrostatic interactions.[184] In their model they considered the stabilizing effect of coulombic interactions between donor and acceptor and the energetic disorder introduced by neighbouring dopant molecules, which opens up delocalisation pathways for polarons. Moreover, a recent study found the effective energy levels of molecular dopants to be strongly affected by electrostatic interactions with the host semiconductor and, hence, measurements of their EA may only provide a limited means for the prediction of charge transfer.[79] In this view, formation of F6TCNNQ dianions with p(a2T-TT), which features an IE ∼4.9 eV that is higher than the EA^- of F6TCNNQ, can be explained by electrostatic interactions. This is in analogy to the report of full charge transfer for doping of pBTTT with F2TCNQ, despite a mismatch of their energy levels.[65] Hence, like for single doping, also for the formation of dopant dianions not only the difference between IE and EA^-, but also electrostatic interactions should be considered.

The electrostatic interactions between an electron hole pair are dependent on the dielectric environment given by the dielectric constant of the surrounding material $\varepsilon = \varepsilon_r\varepsilon_0$, where ε_r is the relative dielectric constant and ε_0 the dielectric constant in vacuum. Typically, organic semiconductors feature relative dielectric constants below 4, which is significantly lower than those of inorganic semiconductors. As a result electron hole pairs tend to be tightly bound to each other and require activation energies in the range of several hundred meV.[204] Especially in the case of organic solar cells enhancing the dielectric

constant of conjugated polymers has been deemed to decrease the binding energy of excitons and in turn increase the solar cell efficiency.[170] Higher dielectric constants are commonly achieved through the addition of fluorine groups[205] or oligoethylene glycol side chains.[206] However, changes of the chemical structure may also lead to unfavourable blend nanostructures resulting in overall lower solar cell performance despite a higher dielectric constant. Constantinou *et al.* recently argued that a high dielectric constant of the neat components is not necessarily crucial to achieve organic solar cells with a high power conversion efficiency. In fact, a higher dielectric environment is already realized by optimizing the nanostructure of donor:acceptor blends allowing enhanced excited state polarizability.[207]

In the case of molecular doping the dielectric environment may influence both the extent of charge transfer and the charge transport. However, experimental investigation presents a considerable challenge since the effective dielectric constant of a (charged) doped layer may differ significantly from that of the neat host semiconductor. Moreover, impedance spectroscopy commonly used to measure the dielectric constant cannot be employed for highly doped layers. For low dopant fractions the influence of a high dielectric constant may directly correlate with an increased doping efficiency as was very recently shown for enhanced n-doping of a high-dielectric fullerene derivative doped with 0.5 mol% N-DMBI.[208]

To investigate whether there is an influence of the dielectric environment on the formation of dopant dianions the relative dielectric constants of pBTTT and p($g_4$2T-TT) were measured by Dr. Hengda Sun at Linköping University using impedance spectroscopy. Indeed, polar tetraethylene glycol side chains in p($g_4$2T-TT) give rise to a higher dielectric constant $\varepsilon_r \sim 4.2$ compared with $\varepsilon_r \sim 2.6$ for pBTTT (paper IV, SI figure 10). A low dielectric constant comparable to that of pBTTT can be expected for p(a2T-TT). Since p(a2T-TT) doped with F6TCNNQ leads to anion formation, whereas doping of p($g_4$2T-TT) with F2TCNQ does not, a higher dielectric constant of the conjugated polymer is

not deemed crucial for dianion formation. Instead, double doping may be significantly more dependent on the electrostatic interactions with charged dopants and polarons. (cf. discussion below).

The dielectric environment may have an effect on the dissociation of ion pairs and hence the delocalisation of polarons in the semiconductor. An indication of the extent of delocalisation of polarons is provided by the position and oscillator strength of two characteristic peaks at 0.15 eV and between 0.3 and 0.6 eV. Charge carrier delocalisation in P3HT was shown to be dependent on the degree of polymer aggregation[127] as well as the donor:acceptor distance[209] influenced by e.g. the use of larger dopant molecules.[89,210] In the case of p($g_4$2T-TT) doped with F4TCNQ a broad peak around 0.4 and 0.5 eV can be observed, which indicates a donor:acceptor distance in the range between 0.6 and 1 nm, corroborated by DFT calculations done by the group of Prof. Adam Moulé at the University of California, Davis (paper IV, SI figures 17 and 18). Additionally, strongly delocalized polarons for molar dopant fractions ≤10 mol% are indicated by a stronger intensity of the peak at 0.15 eV relative to the aforementioned broad peak at higher energies as argued by Ghosh *et al.*[209] The higher dielectric constant of p($g_4$2T-TT) may contribute to the observed strong delocalisation.

Semiconductors and dopants are known to interact in solution. For example, in case of P3HT:F4TCNQ the (electrostatic) interactions between dopant, semiconductor and solvent have been shown to be important for their final film properties.[211] Therefore, I chose to investigate the concentration-dependence of dianion formation in p($g_4$2T-T) doped with a fixed dopant molar ratio of 5 mol% by recording UV-vis spectra at various solute concentration in chloroform/acetonitrile (1:1). Afterwards, the fractions of F4TCNQ anions and dianions were estimated with the previously described fitting procedure (figure 4.10). Spectra were taken after repeated addition of small amounts of a F4TCNQ:p($g_4$2T-T) stock solution and were normalized to their maximum intensity, i.e. the peak associated with the neat polymer at ∼2.1 eV. With increasing concentration of F4TCNQ:p($g_4$2T-T)

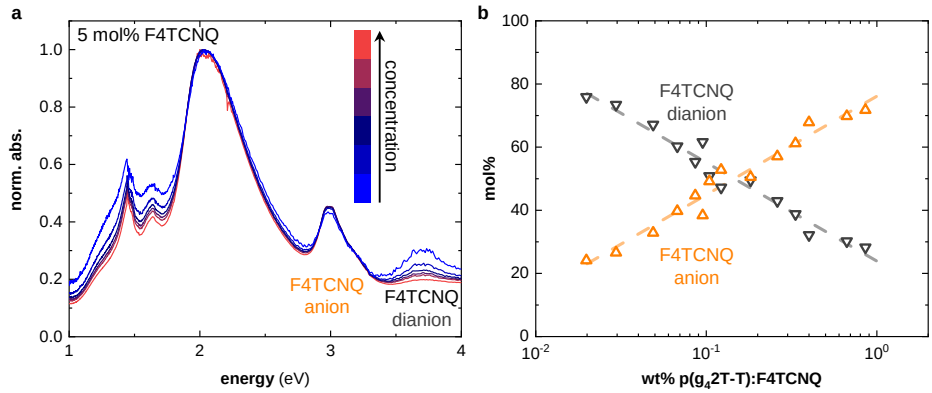

Figure 4.10: *Absorption spectra of p(g$_4$2T-T) doped with 5 mol% F4TCNQ at different solution concentrations (a); molar fractions of F4TCNQ anions and dianions found in p(g$_4$2T-TT) by fitting of UV-vis spectra. (Lines in b are linear fits to the data.)*

the absorption peak of F4TCNQ dianions at ∼3.8 eV decreases with respect to that of anions at ∼2.8 eV, while neutral F4TCNQ is not present. The initial dianion to anion ratio is estimated to be ∼ 4:1, which gradually decreases and finally shifts to a reversed ratio of ∼ 1:4. Despite an overlap of both F4TCNQ anions and polarons below 1.8 eV, the lowered absorption can be ascribed to dedoping of the polymer due to fewer dopant dianions. Hence, F4TCNQ dianions and anions are in a chemical equilibrium similar to the reported equilibrium between neutral and anionic F4TCNQ in P3HT.[57] Note that for higher dopant fractions also neutral F4TCNQ may be present and the complete equilibrium can be stated as follows (P denotes the polymer):

$$\mathrm{F_4TCNQ + P \rightleftharpoons F_4TCNQ^{-} + P^{+} \rightleftharpoons F_4TCNQ^{2-} + P^{++}}$$

Debye-Hückel theory can be used to explain the observed dependence of the equilibrium on the solute concentration. It describes the concentration dependence of solutes in a solvent with the activity of the ionic species, i.e. their ionic radius, and the interactions between them and the solvent.[212,213] In the present system not only the attractive forces

between polarons and dopant anions/dianions, but more importantly the repulsion between F4TCNQ anions and dianions need to be considered. F4TCNQ dianions are assumed to have a larger activity compared with anions since they bear one further negative charge.[214] At low solute concentrations F4TCNQ is dominantly present as dianions since they are sufficiently separated by an average distance of ∼97 nm and can escape the repulsion by other dianions. Instead, for higher concentrations F4TCNQ dianions are forced to be in closer vicinity to neighbouring (charged) F4TCNQ molecules (∼27 nm), whose repelling effect is thought to destabilize dianions and lead to increasingly higher anion fractions. Interestingly, for films of p($g_4$2T-T) doped with the same molar fraction the dianion to anion ratio is found to be ∼ 3:2, which is significantly larger than for high concentrations in solution. This is tentatively ascribed to solid state effects such as aggregation of the polymer. However, electrostatic repulsion between dopant dianions may still be a limiting factor for (double) doping in the solid state. Possible avenues to reduce the repulsive force may be dilution of the polymer with (polar) insulating polymers, similar to F4TCNQ:P3HT:PEO blends, which show an increase in η_{ion} upon addition of PEO (cf. paper I, figure 6), or charge screening by addition of electrolytes.

5 Stability of Molecular Doping

Realisation of commercially-viable organic electronic devices requires that the materials and structures display long-term chemical stability towards a variety of degradation factors, such as light, oxygen, heat, water and chemicals.[215] Specific applications translate into particular requirements like robustness of solar cells towards continuous sun-light exposure, tolerance of elevated temperatures for thermoelectric generators or water- and chemical resistance for bioelectronics. In case of molecular doping the chemical stability of neat semiconductors and dopant molecules as well as that of the doped state need to be considered. Many n-dopants, for example, lack stability towards irreversible oxidation in air and therefore they need to be applied using glove-box techniques ensuring an inert atmosphere. But even n-doping with air-stable molecules such as N-DMBI is known to result in an n-doped state, which is susceptible to the introduction of traps by oxygen and water. These traps rapidly decrease the electrical performance and thus an inert atmosphere is still required. Oxygen may also result in reversible oxidation of p-type semiconductors, i.e. p-doping by electron transfer. The susceptibility of the doped state and neat semiconductors towards oxygen and air is thought to be dependent on their redox potentials.[142] The π-conjugated system in conjugated polymers is also prone to irreversible oxidation by breaking of double bonds and introduction of new groups resulting in shortened conjugation lengths along the backbone and in turn reduced electrical performance.[216] Irreversible oxidation may for example be induced by prolonged heating in ambient air. P-dopants generally display a higher stability towards air compared with n-dopants. However, strong electron acceptors, such as F4TCNQ, display considerable reactivity with e.g. solvents under light exposure.[72] It is commonly understood that their chemical reactivity increases with the EA of the dopant. Small molecular dopants are also known to diffuse through semiconductors, which can cause degradation of electronic devices by migration through different layers, i.e. in OLEDs.[217] The migration of dopant molecules

is enhanced by higher temperatures and electric fields as shown for F4TCNQ.[218,219] Similarly, dopant molecules are prone to sublime from doped layers, which effectively dedopes the semiconductor.[220]

In the context of this thesis the term stability is used to describe the resilience of the electrical conductivity of a material against certain external influences. The first part of this chapter will focus on the thermal stability of p-doped conjugated polymers, whereas the second part will cover the stability of n-doping towards ambient air.

5.1 Thermal Stability of p-Doped Polymers

At elevated temperatures organic semiconductors are prone to degradation by thermal oxidation or thermally induced structural changes and stresses that lead to lowered device performances. Heating of some devices like organic solar cells due to solar radiation is nearly unavoidable and in case of organic thermoelectrics is done intentionally to create a temperature gradient. Therefore, it is important for doped layers to maintain conductivity even upon exposure to thermal stress. Small molecular dopants like F4TCNQ are known to easily sublime at moderate temperatures above ∼80 °C. The high vapour pressure can be exploited for sequential doping of conjugated polymers with dopant vapour (cf. section 2.2).[64,65,74,136] At the same time heating of polymers doped with small molecules results in rapid dedoping as shown for F4TCNQ:P3HT films leading to a drop of their electrical conductivity.[220]

Li *et al.* showed that the thermal stability of doping with F4TCNQ was enhanced for an oligoethylene glycol/sulfonic acid functionalised polythiophene as a result of stronger semiconductor:dopant interactions.[171] In paper II we demonstrate that tetraethylene glycol side chains help to maintain the electrical conductivity of p($g_4$2T-T) doped with F4TCNQ up to 150 °C. Here, additional UV-vis spectra at elevated temperatures and

data for p($g_4$2T-TT) are added to the analysis of the thermal stability of polythiophenes with oligoethylene glycol side chains.

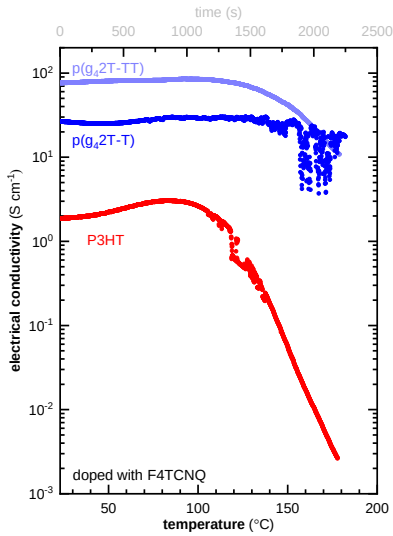

Figure 5.1: *Electrical conductivity of p($g_4$2T-TT), p($g_4$2T-T) and P3HT doped with F4TCNQ during gradual heating. Note that p($g_4$2T-T) and P3HT are doped with* 10 mol% *per thiophene (*12.3 *and* 15.6 wt%*) and p($g_4$2T-TT) is doped with* 40 mol% *relative to the polymer repeat unit (*20.5 wt%*).*

To follow the temperature-dependence of the electrical conductivity of p($g_4$2T-T), p($g_4$2T-TT) and P3HT doped with F4TCNQ, thin drop-cast films were gradually heated from room temperature to 180 °C at 2 °C min^{-1} and at ambient atmosphere (figure 5.1). The two polymers bearing tetraethylene glycol side chains display a markedly different behaviour compared with P3HT. The electrical conductivity of doped P3HT drastically drops by several orders of magnitude. The onset of the drop at ∼80 °C is in agreement with Hase *et al.* who reported the electrical conductivity of of thin spin-coated films of F4TCNQ:P3HT after static temperature annealing for 60 min.[220] Instead, p($g_4$2T-T) doped with the same molar fraction displays near constant conductivity until up to ∼150 °C, which is explained with significantly slower sublimation of F4TCNQ from p($g_4$2T-TT) as compared with

P3HT (paper II, SI figure 13). The conductivity of p($g_4$2T-TT) also remains constant up to ∼120 °C and then slowly decreases, which may be a result of the higher dopant weight fraction of 20.5 wt% compared with doped films of p($g_4$2T-T) that contained only 12.3 wt% F4TCNQ. The enhanced thermal stability of p($g_4$2T-T) and p($g_4$2T-TT) compared with P3HT is rationalized with electrostatic interactions through dipole-dipole forces between F4TCNQ and the tetraethylene glycol side chains (cf. chapter 3). This is in agreement with the study of bilayers consisting of an oligoethylene glycol functionalized polythiophene and P3HT by Li *et al.* where F4TCNQ was found to preferably reside in the polar polythiophene layer.[171] Reduced side chain density, which increases the available space for dopant ions, may also contribute to the observed behaviour.[221] High thermal stability was recently also demonstrated by Hofmann *et al.* for doping of p($g_4$2T-T) with several organic acids.[95]

Dopant molecules and conjugated polymers are in an equilibrium with their charged species (cf sections 4.1.2 and 4.2). Wang *et al.* found that the equilibrium in F4TCNQ:P3HT is temperature dependent and heating and cooling of solutions resulted in reversible (de)doping.[222] To probe the temperature-dependence of double doping I recorded spectra of drop-cast films at different temperatures and estimated the fractions of abundant F4TCNQ species by fitting according to the procedure described in paper IV. For a low dopant molar fraction of 2 mol% (figure 5.2) a large fraction of F4TCNQ dianions $x_{dianion} > 95\,\%$ and complete absence of neutral F4TCNQ is estimated for as spin-coated films at 20 °C. Increasing the temperature by steps of 20 °C to a final temperature of 100 °C resulted in fewer F4TCNQ dianions concomitant with a higher fraction of dopant anions $x_{anion} \sim 40\,\%$. Simultaneously, spectral features associated with the neutral polymer slightly increase and the absorption below ∼1.7 eV decreases indicating a smaller number of polarons in agreement with fewer dopant dianions. Cooling to the starting temperature recovers the initial ratio between anions and dianions. However, the total number of F4TCNQ anions and dianions is reduced, which may be explained with slow

sublimation of dopant from the film by continuous heating for a prolonged time during the measurements.

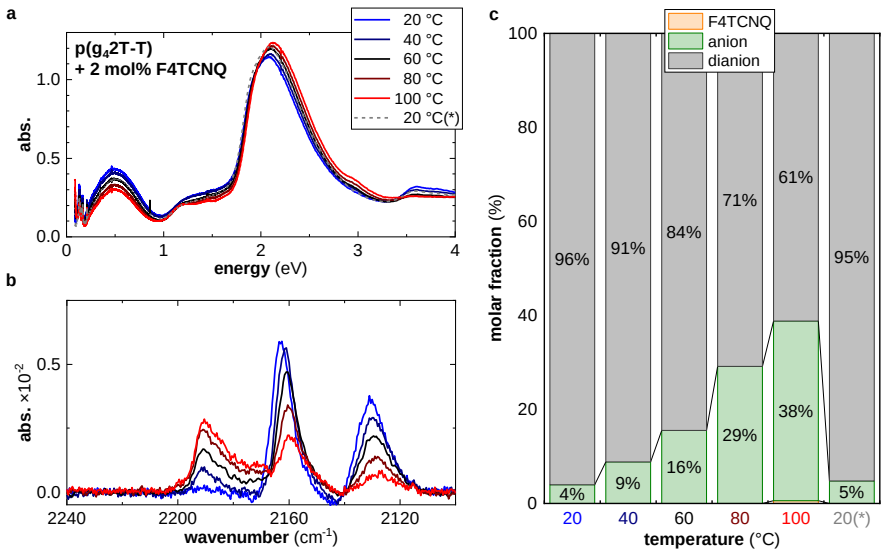

Figure 5.2: *UV-vis (a) and FTIR (b) absorption spectra of p($g_4$2T-T) doped with* 2 mol% *and molar fractions of neat and anionic F4TCNQ at various temperatures (c).*
(*) Temperature after cooling.

For films doped with a higher molar fraction of 10 mol% F4TCNQ only neat and anionic F4TCNQ, but not dianions can be discerned (figure 5.3). Heating results in an increasing relative fraction of anions to neutral F4TCNQ from $x_{anion} \sim 44\,\%$ at 20 °C to ∼80 % for 100 °C. This is associated with a marginally decrease of the polaron absorption and slightly higher neat polymer absorption. Relative fractions of anionic and neat F4TCNQ after cooling are comparable to their initial values, but similar to films containing a low dopant fraction the total amount of dopant molecules is found to be reduced and may again be explained by sublimation of F4TCNQ. Dopant sublimation may also account for the discrepancy between lowered polaron absorption and increased anion fraction at higher temperatures ≤80 °C. Polaron absorption below 1 eV is also strongly influenced

by changes to the charge carrier delocalisation, which may play a role for the observed behaviour.[209]

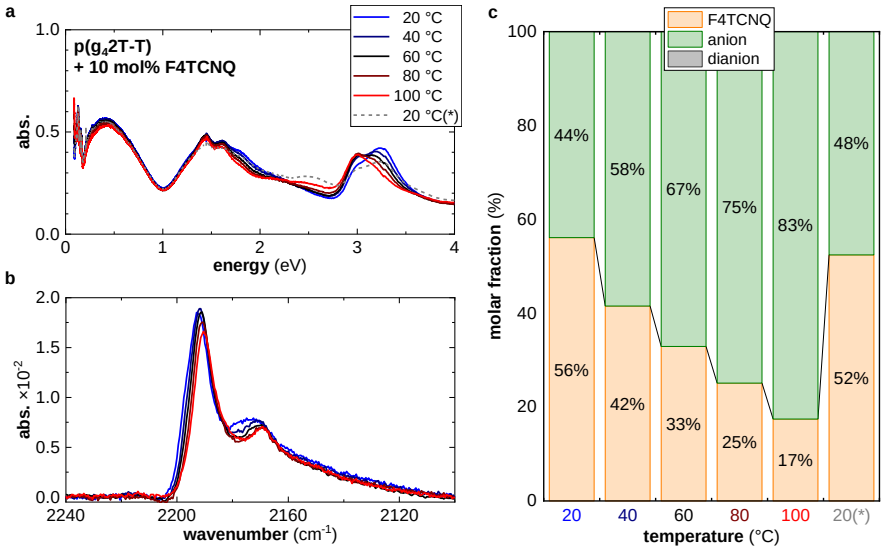

Figure 5.3: *UV-vis (a) and FTIR (b) absorption spectra of p($g_4$2T-T) doped with* 10 mol% *and molar fractions of neat and anionic F4TCNQ at various temperatures (c).*
(*) Temperature after cooling.

Finally, I investigated the thermal stability of p($g_4$2T-T) doped with a set of different molecular dopants by annealing for 5 min at elevated temperatures (figure 5.4). The set of dopants include bulky molecules, such as the fluorinated fullerene $C_{60}F_{48}$ supplied by Dr. Olga Boltalina, Colorado State University, and several molybdenum metal complexes from Prof. Seth Marder's group at Georgia Institute of Technology, which are not prone to sublimation. For all dopants except of F6TCNNQ a drop of the film conductivity is observed between 100 and 130 °C. Instead, for F6TCNNQ a conductivity drop is only noted after annealing at 160 °C, which may be attributed to a reduced vapour pressure compared with F4TCNQ. Note that thin spin-coated films were used for this analysis, which may favour the sublimation of F4TCNQ and thus explaining the earlier loss of electrical conductivity as compared with gradual heating, where thicker drop-cast films

were investigated (cf. figure 5.1). For small, light dopants such as TCNQ and TCNE sublimation may be responsible for the loss of electrical conductivity after exposure to higher temperatures. Bulky, heavy dopants lack the ability to sublime and hence it can be excluded as a cause for their loss of conductivity. Even for small dopant molecules sublimation is likely not the only cause for the observed temperature instability. Possible other explanations may be changes to the nanostructure of doped films, e.g. phase separation of the dopant, or chemical reactions that may involve both the ionized semiconductor and the dopant, e.g. thermal oxidation. Other chemical reaction besides oxidation are also indicated in the case of P3HT:F4TCNQ, where I noted the occurrence of a strong exothermic peak below 190 °C in differential scanning calorimetry in inert atmosphere, which implies a chemical reaction between the dopant and the semiconductor. Furthermore, the results demonstrate that very short annealing times of only 5 min at elevated temperatures are sufficient to significantly reduce the conductivity of thin films of doped conjugated polymers.

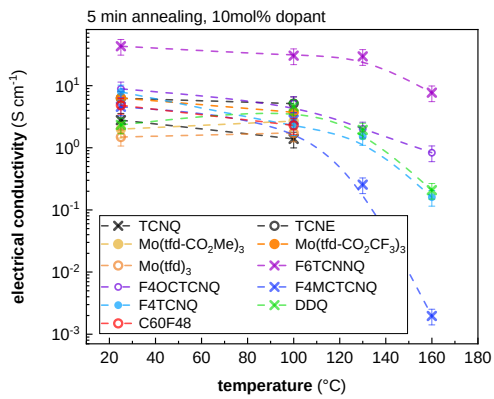

Figure 5.4: *Electrical conductivity of p($g_4$2T-T) doped with* 10 mol% *of several different molecular dopants of as spin-coated films and after annealing for* 5 min *at* 100, 130 *and* 160 °C. *Missing data points indicate that the conductivity dropped below the measurable range. Preparation of films and electrical measurements were undertaken by Dr. Anna Hofmann and myself.*

In general, there are many pathways by which thermal degradation can occur and therefore dopant:semiconductor pairs need to be considered individually. Further, they may be depend on the incorporated amount of dopant and the sample dimensions. In case of p($g_4$2T-T) doped with F4TCNQ, dopant ionisation is found to be strongly temperature dependent. The relative amounts of neutral, anionic and dianionic F4TCNQ were found to reversibly change upon heating to 100 °C. Polar oligoethylene glycol side chains offer significantly improved thermal stability compared with P3HT, as a result of enhanced interactions with F4TCNQ. Possible strategies for further improvement of the thermal stability of doped conjugated polymers include the use of bulkier dopants that are less prone to sublimation or chemical linking of dopants by either cross-linking or tethering to the side chains, i.e. self-doping. Note that the doped state may still be vulnerable to thermal oxidation, which may require different solutions, e.g. encapsulation.

5.2 Air Stability of n-Doped Polymers

N-doped organic semiconductors are needed for the operation of nearly all types of organic electronic devices, like as active material in organic thermoelectric generators or as interlayers in organic solar cells and OLEDs (cf. chapter 2). However, n-doped organic semiconductors commonly suffer from rapid loss of their conductivity when exposed to air. N-type organic layers are thought to be passivated by electron trapping induced by oxygen and water molecules.[142,223,224] Encapsulation is a common way to protect from water and oxygen, but intrinsic solutions for better air stability are required. The most promising approach is to decrease the LUMO level, i.e. to increase the EA, of semiconductors by electron withdrawing groups, which has been demonstrated for several small molecular semiconductors.[225–228] This principle was expanded to conjugated polymers[229,230] and very recently Nava *et al.* reported air stable n-doping of the thiolated conjugated polymer 2S-*trans*-PNDIT2 previously mentioned in chapter 2. Compared with

its analogue p(NDI2OD-T2) it features an increased EA, which is thought to reduce the redox-activity of electrons induced by the dopant N-DPBI. The authors found a remarkable stability of the electrical conductivity for continuous exposure to air, whereas that of p(NDI2OD-T2) rapidly decreased.

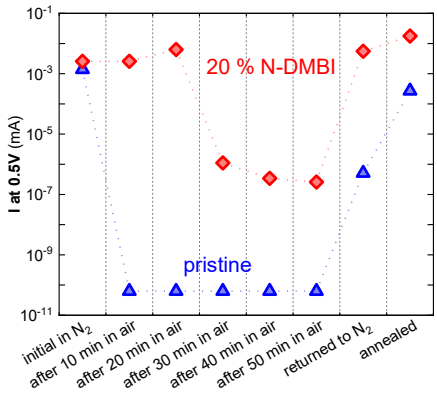

Figure 5.5: *Air stability of pristine and N-DMBI-doped p(gNDI-gT2); the current at* 0.5 V *was extracted from I–V curves recorded in nitrogen, in air, and finally again in nitrogen. Note that the non-ohmic behaviour of several samples prevented us from extracting the electrical conductivity.*

Air stability measurements of p(gNDI-gT2) displayed in figure 5.5 were undertaken by Dr. Hengda Sun and myself at Linköping University. Freshly prepared films of neat and doped p(gNDI-gT2) were exposed to ambient air and the current-voltage (I-V) behaviour was recorded at various times (paper IV, SI figure 13). We chose to use the current measured at 0.5 V because of non-ohmic behaviour of doped samples after air exposure for 30 min, which prohibited extraction of the electrical conductivity. The response of neat and doped samples to air exposure was significantly different. The current for neat films rapidly dropped by several orders of magnitude upon air exposure. Instead, the current measured for doped films remained similar for the first 20 min and then decreased significantly. Interestingly, returning the samples to the glovebox followed by annealing at 80 °C for 10 min recovered the current for both samples. This behaviour suggests that passivation

takes place by absorption of oxygen or water from air, which is further indicated by a reduced conductivity after intentional exposure of the film to water (paper IV, SI figure 14). In fact, the susceptibility of water absorption by polar side chains was recently demonstrated by Savva *et al.*[231] The results further indicate that doped samples can be handled in ambient atmosphere for a short period of time. A better air stability of p(gNDI-gT2) could be expected due to its higher EA of ∼4.1 eV[166] compared with e.g. p(NDI2OD-T2) (∼4.0 eV[174]). However, p(gNDI-gT2) also features a low IE of ∼4.8 eV as a result of the electron-rich thiophene units, which induces susceptibility to oxidation by ambient oxygen and may lead to less mobile polarons by localisation on NDI units.

To allow both air-stable doping and good miscibility of dopants with conjugated polymers, thionated structures used by Nava et al.[144] could be combined with the addition of glycol side chains. Alkyl spacers between the backbone and the ethylene glycol units should be used in order to avoid the reduction of the IE.

6 Concluding Remarks & Outlook

Several strategies to enhance the efficiency and stability of molecular doping of conjugated polymers were discussed in this thesis. To begin with I investigated blending of a doped conjugated polymer with insulator polymers to fabricate conducting bulk structures. Unfortunately, processing of F4TCNQ:P3HT with PEO, PLLA and PE was found to not significantly improve processing of the doped semiconductor. Nonetheless, good compatibility of PEO with F4TCNQ:P3HT was observed, which was ascribed to the polarity of PEO. Encouraged by this first study I explored the effect of polar oligoethylene glycol side chains instead of alkyl side chains on molecular doping. Polar side chains were found to significantly enhance the compatibility of both n- and p-type conjugated polymers with polar molecular dopants and their solubility in polar organic solvents. Films of p($g_4$2T-T) bearing tetraethylene glycol side chains p-doped with F4TCNQ could be cast at room temperature and did not suffer from excess dopant interrupting their nanostructure at saturated dopant loadings as opposed to F4TCNQ-doped P3HT, which carries alkyl side chains. Likewise, phase separation of the n-dopant N-DMBI and the conjugated polymer p(gNDI-gT2) was largely suppressed up to a dopant molar ratio of 20 mol% by its oligoethylene glycol based side chains. The good compatibility led to a ten times higher ionisation efficiency in doped p(gNDI-gT2) of 13 % compared with its analogue p(NDI2OD-T2), which gave rise to a higher electrical conductivity of $0.3\,\mathrm{S\,cm^{-1}}$.

Secondly, I studied the impact of lowering the IE of p-type conjugated polymers on molecular doping and discussed the electrostatic interactions between the semiconductor and dopant. A lower IE allows a greater choice of dopant molecules as demonstrated by efficient doping of p($g_4$2T-T) with the weak dopant DDQ. More importantly, a low IE was found to give rise to the novel concept of double doping, where the transfer of

two electrons from a conjugated polymer to a single dopant molecule leads to formation of dopant dianions. The common molecular dopant F4TCNQ readily forms dianions in p($g_4$2T-TT), which results in twice as many charge carriers on the conjugated polymer and allows to significantly reduce the dopant fraction. I demonstrated the formation of dopant dianions for nine different conjugated polymer / dopant combinations, which illustrates that dianion formation in conjugated polymers is a general concept. Double doping is favoured by an offset between the IE of the conjugated polymer and the EA^0 of the molecular dopant as well as the EA^- of its corresponding anion. Favourable electrostatic interactions between dopant and semiconductor are likely a further factor that impacts dopant dianion formation. Furthermore, the equilibrium between neutral and charged dopant and conjugated polymer was found to depend on their concentration, which was correlated with electrostatic interactions between the charged species.

Finally, the thermal stability of p-doped p($g_4$2T-T) and p($g_4$2T-TT) and the air-stability of n-doped p(gNDI-gT2) were studied. The polar side chains were demonstrated to significantly increase the thermal stability compared with P3HT. Prolonged heating was found to reduce the amount of F4TCNQ in p($g_4$2T-T), which may be partially due to dopant sublimation. However, other degradation mechanisms e.g. thermal oxidation could not be excluded. N-doped films of p(gNDI-gT2) were found to be stable in air for a short time after which their conduction strongly decreased, which could be reversed through annealing in inert atmosphere. This behaviour was ascribed to introduction of reversible traps by oxygen or water in air.

The results presented in this thesis will aid the design of highly efficient, solution-processable and highly conducting molecularly doped conjugated polymers that are in high demand for a wide range of applications. Polar side chains are particularly interesting for printing of doped conjugated polymers and for bulk processing, where sequential doping is not applicable. To further advance the use of polar conjugated polymers for molecular doping it is necessary to understand the impact of processing methods and the

resulting underlying nanostructure on their properties. These may not be simply conveyed from conjugated polymer with aliphatic side chains. One can envision a large variety of conjugated polymers with different polar side chain structures adapted to the desired solvent, dopant and post-treatment.

The concept of double doping constitutes a significant improvement for molecular doping of conjugated polymers since it may allow to considerably reduce the number of dopant molecules that is required to reach a high electrical conductivity. This thesis provides some initial design criteria for conjugated polymers that are needed to enable dopant dianion formation of strong two-electron acceptor molecular dopants. I anticipate that the design of polymers with higher charge-carrier mobility and energy levels designed for double doping as well as the use of stronger dopants with the ability to abstract two electrons from polymers with a higher IE will result in a new class of highly conducting materials. To fully harness double doping it will be important to gain a comprehensive picture of how the chemical structure and underlying nanostructures, such as aggregation, influence dopant dianion formation. This may in part be aided by revisiting existing literature, where dopant dianions may be present, but have not been noticed. Double doping may theoretically also be applicable for the design of n-doped conjugated polymers through formation of dopant dications. However, potential structures for dopant molecules with a sufficiently low IE are predicted to be extremely unstable. In particular for organic thermoelectrics it will be important to understand the mechanisms that lead to thermal degradation in molecularly doped conjugated semiconductors. It is clear that polar interactions between dopant and conjugated polymer and dopants with a higher molecular weight are important factors that impact the tendency of the dopant to sublime. However, evidently there are other degradation pathways that play a role and must be addressed. In summary, in my thesis I have shown that polar side chains are a powerful design tool that allows to enhance the processability, doping efficiency and stability of doped conjugated polymers.

Bibliography

[1] J. Bardeen and W. H. Brattain, *Phys. Rev.* **1948**, 74 (2), 230–231.

[2] H. Shirakawa, E. J. Louis, A. G. MacDiarmid, C. K. Chiang and A. J. Heeger, *J. Chem. Soc., Chem. Commun.* **1977**, – (16), 578–580.

[3] C. W. Tang and S. A. VanSlyke, *Appl. Phys. Lett.* **1987**, 51 (12), 913–915.

[4] J. H. Burroughes, D. D. C. Bradley, A. R. Brown, R. N. Marks, K. Mackay, R. H. Friend, P. L. Burn and A. B. Holmes, *Nature* **1990**, 347 (6293), 539–541.

[5] C. W. Tang, *Appl. Phys. Lett.* **1986**, 48 (2), 183–185.

[6] J. J. M. Halls, C. A. Walsh, N. C. Greenham, E. A. Marseglia, R. H. Friend, S. C. Moratti and A. B. Holmes, *Nature* **1995**, 376 (6540), 498–500.

[7] G. Yu, J. Gao, J. C. Hummelen, F. Wudl and A. J. Heeger, *Science* **1995**, 270 (5243), 1789–1791.

[8] The Royal Swedish Academy of Sciences, The Nobel Prize in Chemistry, 2000: Conductive polymers, Online press release: `https://www.nobelprize.org/prizes/chemistry/2000/summary/`, accessed 08-Apr-2019.

[9] S. Forrest, P. Burrows and M. Thompson, *IEEE Spectr.* **2000**, 37 (8), 29–34.

[10] A. Salleo, F. Cicoira and C. Santato (Editors), *Organic Electronics: Emerging Concepts and Technologies*, 1 edition, chapter 14 Electronic Traps in Organic Semiconductors, John Wiley & Sons, Incorporated, Weinheim, GERMANY, **2013**, 341–380.

[11] OLED lighting introduction and market status, URL: `https://www.oled-info.com/oled-lighting`, accessed: 08-Apr-2019.

[12] Three ways organic electronics is changing technology as we know it, URL: `http://theconversation.com/three-ways-organic-electronics-is-changing-technology-as-we-know-it-63287`, accessed 08-Apr-2019.

[13] Plastic Logic GmbH, URL: `https://www.plasticlogic.com/`, accessed 08-Apr-2019.

[14] Y. H. Lee, M. Jang, M. Y. Lee, O. Y. Kweon and J. H. Oh, *Chem* **2017**, 3 (5), 724–763.

[15] T. Sekitani, U. Zschieschang, H. Klauk and T. Someya, *Nat. Mater.* **2010**, 9 (12), 1015–1022.

[16] D. D. C. Rasi and R. A. J. Janssen, *Adv. Mater.* **2018**, 31 (10), 1806499.

[17] R. Kroon, D. A. Mengistie, D. Kiefer, J. Hynynen, J. D. Ryan, L. Yu and C. Müller, *Chem. Soc. Rev.* **2016**, 45 (22), 6147–6164.

[18] B. Russ, A. Glaudell, J. J. Urban, M. L. Chabinyc and R. A. Segalman, *Nat. Rev. Mater.* **2016**, 1 (10), 16050.

[19] S. Muench, A. Wild, C. Friebe, B. Häupler, T. Janoschka and U. S. Schubert, *Chem. Rev.* **2016**, 116 (16), 9438–9484.

[20] J. Rivnay, R. M. Owens and G. G. Malliaras, *Chem. Mater.* **2013**, 26 (1), 679–685.

[21] G. G. Malliaras, *Biochim. Biophys. Acta. Gen. Subj.* **2013**, 1830 (9), 4286–4287.

[22] U. N. Maiti, W. J. Lee, J. M. Lee, Y. Oh, J. Y. Kim, J. E. Kim, J. Shim, T. H. Han and S. O. Kim, *Adv. Mater.* **2013**, 26 (1), 40–67.

[23] A. D. Jenkins, P. Kratochvíl, R. F. T. Stepto and U. W. Suter, *Pure and Appl. Chem.* **2009**, 68 (12), 2287–2311.

[24] C. Liu, K. Wang, X. Gong and A. J. Heeger, *Chem. Soc. Rev.* **2016**, 45 (17), 4825–4846.

[25] D. Gedefaw, M. Prosa, M. Bolognesi, M. Seri and M. R. Andersson, *Adv. Energy Mater.* **2017**, 7 (21), 1700575.

[26] C. Müller, *Chem. Mater.* **2015**, 27 (8), 2740–2754.

[27] F. P. V. Koch, J. Rivnay, S. Foster, C. Müller, J. M. Downing, E. Buchaca-Domingo, P. Westacott, L. Yu, M. Yuan, M. Baklar, Z. Fei, C. Luscombe, M. A. McLachlan, M. Heeney, G. Rumbles, C. Silva, A. Salleo, J. Nelson, P. Smith and N. Stingelin, *Prog. Polym. Sci.* **2013**, 38 (12), 1978–1989.

[28] C.-K. Mai, R. A. Schlitz, G. M. Su, D. Spitzer, X. Wang, S. L. Fronk, D. G. Cahill, M. L. Chabinyc and G. C. Bazan, *J. Am. Chem. Soc.* **2014**, 136 (39), 13478–13481.

[29] I. McCulloch, M. Heeney, C. Bailey, K. Genevicius, I. MacDonald, M. Shkunov, D. Sparrowe, S. Tierney, R. Wagner, W. Zhang, M. L. Chabinyc, R. J. Kline, M. D. McGehee and M. F. Toney, *Nat. Mater.* **2006**, 5 (4), 328–333.

[30] K. Walzer, B. Maennig, M. Pfeiffer and K. Leo, *Chem. Rev.* **2007**, 107 (4), 1233–1271.

[31] B. Lüssem, C.-M. Keum, D. Kasemann, B. Naab, Z. Bao and K. Leo, *Chem. Rev.* **2016**, 116 (22), 13714–13751.

[32] A. Lund, N. M. van der Velden, N.-K. Persson, M. M. Hamedi and C. Müller, *Mater. Sci. Eng. R Rep.* **2018**, 126, 1–29.

[33] A. J. Heeger, N. S. Sariciftci and E. B. Namdas, *Semiconducting and Metallic Polymers*, Oxford University Press, **2010**.

[34] Arramel, H. Pan, A. Xie, S. Hou, X. Yin, C. S. Tang, N. T. Hoa, M. D. Birowosuto, H. Wang, C. Dang, A. Rusydi, A. T. S. Wee and J. Wu, *Nano Res.* **2018**, 12 (1), 77–84.

[35] M. Makkar and R. Viswanatha, *RSC Adv.* **2018**, 8 (39), 22103–22112.

[36] C. Han and R. Elsenbaumer, *Synth. Met.* **1989**, 30 (1), 123–131.

[37] I. E. Jacobs and A. J. Moulé, *Adv. Mater.* **2017**, 29 (42), 1703063.

[38] I. Salzmann, G. Heimel, M. Oehzelt, S. Winkler and N. Koch, *Acc. Chem. Res.* **2016**, 49 (3), 370–378.

[39] G. C. Welch and G. C. Bazan, *J. Am. Chem. Soc.* **2011**, 133 (12), 4632–4644.

[40] G. C. Welch, R. Coffin, J. Peet and G. C. Bazan, *J. Am. Chem. Soc.* **2009**, 131 (31), 10802–10803.

[41] Y. Han, Z. Fei, Y.-H. Lin, J. Martin, F. Tuna, T. D. Anthopoulos and M. Heeney, *npj Flex. Electron.* **2018**, 2 (1), 11.

[42] X. Zhao, D. Madan, Y. Cheng, J. Zhou, H. Li, S. M. Thon, A. E. Bragg, M. E. DeCoster, P. E. Hopkins and H. E. Katz, *Adv. Mater.* **2017**, 29 (34), 1606928.

[43] J. L. Bredas and G. B. Street, *Acc. Chem. Res.* **1985**, 18 (10), 309–315.

[44] G. Heimel, *ACS Central Sci.* **2016**, 2 (5), 309–315.

[45] S. Winkler, P. Amsalem, J. Frisch, M. Oehzelt, G. Heimel and N. Koch, *Mater. Horiz.* **2015**, 2 (4), 427–433.

[46] R.-Q. Png, M. C. Ang, M.-H. Teo, K.-K. Choo, C. G. Tang, D. Belaineh, L.-L. Chua and P. K. Ho, *Nat. Commun.* **2016**, 7 (1), 11948.

[47] I. Zozoulenko, A. Singh, S. K. Singh, V. Gueskine, X. Crispin and M. Berggren, *ACS Appl. Polymer Mater.* **2018**, 1 (1), 83–94.

[48] H. C. F. Martens, I. N. Hulea, I. Romijn, H. B. Brom, W. F. Pasveer and M. A. J. Michels, *Phys. Rev. B* **2003**, 67 (12), 121203(R).

[49] Y. Nogami, H. Kaneko, T. Ishiguro, A. Takahashi, J. Tsukamoto and N. Hosoito, *Solid State Commun.* **1990**, 76 (5), 583–586.

[50] M. Rolland, S. Lefrant, M. Aldissi, P. Bernier, E. Rzepka and F. Schue, *J. Electron. Mater.* **1981**, 10 (4), 619–630.

[51] D. Kiefer, R. Kroon, A. I. Hofmann, H. Sun, X. Liu, A. Giovannitti, D. Stegerer, A. Cano, J. Hynynen, L. Yu, Y. Zhang, D. Nai, T. F. Harrelson, M. Sommer, A. J. Moulé, M. Kemerink, S. R. Marder, I. McCulloch, M. Fahlman, S. Fabiano and C. Müller, *Nat. Mater.* **2019**, 18 (2), 149–155.

[52] J. Li, G. Zhang, D. M. Holm, I. E. Jacobs, B. Yin, P. Stroeve, M. Mascal and A. J. Moulé, *Chem. Mater.* **2015**, 27 (16), 5765–5774.

[53] E. Lim, B.-J. Jung, M. Chikamatsu, R. Azumi, Y. Yoshida, K. Yase, L.-M. Do and H.-K. Shim, *J. Mater. Chem.* **2007**, 17 (14), 1416.

[54] K.-H. Yim, G. L. Whiting, C. E. Murphy, J. J. M. Halls, J. H. Burroughes, R. H. Friend and J.-S. Kim, *Adv. Mater.* **2008**, 20 (17), 3319–3324.

[55] P. Pingel, R. Schwarzl and D. Neher, *Appl. Phys. Lett.* **2012**, 100 (14), 143303.

[56] P. Pingel and D. Neher, *Phys. Rev. B* **2013**, 87 (11), 115209.

[57] D. T. Duong, C. Wang, E. Antono, M. F. Toney and A. Salleo, *Org. Electron.* **2013**, 14 (5), 1330–1336.

[58] J. Gao, J. D. Roehling, Y. Li, H. Guo, A. J. Moulé and J. K. Grey, *J. Mater. Chem. C* **2013**, 1 (36), 5638.

[59] J. Gao, E. T. Niles and J. K. Grey, *J. Phys. Chem. Lett.* **2013**, 4 (17), 2953–2957.

[60] D. T. Duong, H. Phan, D. Hanifi, P. S. Jo, T.-Q. Nguyen and A. Salleo, *Adv. Mater.* **2014**, 26 (35), 6069–6073.

[61] H. Méndez, G. Heimel, S. Winkler, J. Frisch, A. Opitz, K. Sauer, B. Wegner, M. Oehzelt, C. Röthel, S. Duhm, D. Többens, N. Koch and I. Salzmann, *Nat. Commun.* **2015**, 6 (1), 8560.

[62] J. E. Cochran, M. J. N. Junk, A. M. Glaudell, P. L. Miller, J. S. Cowart, M. F. Toney, C. J. Hawker, B. F. Chmelka and M. L. Chabinyc, *Macromolecules* **2014**, 47 (19), 6836–6846.

[63] A. M. Glaudell, J. E. Cochran, S. N. Patel and M. L. Chabinyc, *Adv. Energy Mater.* **2014**, 5 (4), 1401072.

[64] K. Kang, S. Watanabe, K. Broch, A. Sepe, A. Brown, I. Nasrallah, M. Nikolka, Z. Fei, M. Heeney, D. Matsumoto, K. Marumoto, H. Tanaka, S. Kuroda and H. Sirringhaus, *Nat. Mater.* **2016**, 15 (8), 896–902.

[65] S. N. Patel, A. M. Glaudell, K. A. Peterson, E. M. Thomas, K. A. O'Hara, E. Lim and M. L. Chabinyc, *Sci. Adv.* **2017**, 3 (6), e1700434.

[66] S. Yoon, J. Cho, H.-K. Lee, S. Park, H. J. Son and D. S. Chung, *Appl. Phys. Lett.* **2015**, 107 (13), 133302.

[67] Y. Karpov, T. Erdmann, I. Raguzin, M. Al-Hussein, M. Binner, U. Lappan, M. Stamm, K. L. Gerasimov, T. Beryozkina, V. Bakulev, D. V. Anokhin, D. A. Ivanov, F. Günther, S. Gemming, G. Seifert, B. Voit, R. D. Pietro and A. Kiriy, *Adv. Mater.* **2016**, 28 (28), 6003–6010.

[68] I. E. Jacobs, C. Cendra, T. F. Harrelson, Z. I. B. Valdez, R. Faller, A. Salleo and A. J. Moulé, *Mater. Horiz.* **2018**, 5 (4), 655–660.

[69] D. T. Scholes, S. A. Hawks, P. Y. Yee, H. Wu, J. R. Lindemuth, S. H. Tolbert and B. J. Schwartz, *J. Phys. Chem. Lett.* **2015**, 6 (23), 4786–4793.

[70] I. E. Jacobs, E. W. Aasen, J. L. Oliveira, T. N. Fonseca, J. D. Roehling, J. Li, G. Zhang, M. P. Augustine, M. Mascal and A. J. Moulé, *J. Mater. Chem. C* **2016**, 4 (16), 3454–3466.

[71] J. Fuzell, I. E. Jacobs, S. Ackling, T. F. Harrelson, D. M. Huang, D. Larsen and A. J. Moulé, *J. Phys. Chem. Lett.* **2016**, 7 (21), 4297–4303.

[72] I. E. Jacobs, E. W. Aasen, D. Nowak, J. Li, W. Morrison, J. D. Roehling, M. P. Augustine and A. J. Moulé, *Adv. Mater.* **2016**, 29 (2), 1603221.

[73] J. Li, D. M. Holm, S. Guda, Z. I. Bedolla-Valdez, G. Gonel, I. E. Jacobs, M. A. Dettmann, J. Saska, M. Mascal and A. J. Moulé, *J. Mater. Chem. C* **2019**, 7 (2), 302–313.

[74] J. Hynynen, D. Kiefer, L. Yu, R. Kroon, R. Munir, A. Amassian, M. Kemerink and C. Müller, *Macromolecules* **2017**, 50 (20), 8140–8148.

[75] J. Hynynen, D. Kiefer and C. Müller, *RSC Adv.* **2018**, 8 (3), 1593–1599.

[76] A. Hamidi-Sakr, L. Biniek, J.-L. Bantignies, D. Maurin, L. Herrmann, N. Leclerc, P. Lévêque, V. Vijayakumar, N. Zimmermann and M. Brinkmann, *Adv. Funct. Mater.* **2017**, 27 (25), 1700173.

[77] I. Salzmann, G. Heimel, S. Duhm, M. Oehzelt, P. Pingel, B. M. George, A. Schnegg, K. Lips, R.-P. Blum, A. Vollmer and N. Koch, *Phys. Rev. Lett.* **2012**, 108 (3), 035502.

[78] H. Kleemann, C. Schuenemann, A. A. Zakhidov, M. Riede, B. Lüssem and K. Leo, *Org. Electron.* **2012**, 13 (1), 58–65.

[79] J. Li, I. Duchemin, O. M. Roscioni, P. Friederich, M. Anderson, E. D. Como, G. Kociok-Köhn, W. Wenzel, C. Zannoni, D. Beljonne, X. Blase and G. D'Avino, *Mater. Horiz.* **2019**, 6 (1), 107–114.

[80] F. Ghani, A. Opitz, P. Pingel, G. Heimel, I. Salzmann, J. Frisch, D. Neher, A. Tsami, U. Scherf and N. Koch, *J. Polym. Sci., Part B: Polym. Phys.* **2014**, 53 (1), 58–63.

[81] P. Pingel, L. Zhu, K. S. Park, J.-O. Vogel, S. Janietz, E.-G. Kim, J. P. Rabe, J.-L. Brédas and N. Koch, *J. Phys. Chem. Lett.* **2010**, 1 (13), 2037–2041.

[82] D. D. Nuzzo, C. Fontanesi, R. Jones, S. Allard, I. Dumsch, U. Scherf, E. von Hauff, S. Schumacher and E. D. Como, *Nat. Commun.* **2015**, 6 (1), 6460.

[83] H. Méndez, G. Heimel, A. Opitz, K. Sauer, P. Barkowski, M. Oehzelt, J. Soeda, T. Okamoto, J. Takeya, J.-B. Arlin, J.-Y. Balandier, Y. Geerts, N. Koch and I. Salzmann, *Angew. Chem. Int. Ed.* **2013**, 52 (30), 7751–7755.

[84] Y. Qi, T. Sajoto, M. Kröger, A. M. Kandabarow, W. Park, S. Barlow, E.-G. Kim, L. Wielunski, L. C. Feldman, R. A. Bartynski, J.-L. Brédas, S. R. Marder and A. Kahn, *Chem. Mater.* **2010**, 22 (2), 524–531.

[85] A. Dai, Y. Zhou, A. L. Shu, S. K. Mohapatra, H. Wang, C. Fuentes-Hernandez, Y. Zhang, S. Barlow, Y.-L. Loo, S. R. Marder, B. Kippelen and A. Kahn, *Adv. Funct. Mater.* **2013**, 24 (15), 2197–2204.

[86] J. Hynynen, E. Järsvall, R. Kroon, Y. Zhang, S. Barlow, S. R. Marder, M. Kemerink, A. Lund and C. Müller, *ACS Macro Lett.* **2018**, 8 (1), 70–76.

[87] J. Euvrard, A. Revaux, S. S. Nobre, A. Kahn and D. Vuillaume, *J. Appl. Phys.* **2018**, 123 (22), 225501.

[88] J. Euvrard, A. Revaux, P.-A. Bayle, M. Bardet, D. Vuillaume and A. Kahn, *Org. Electron.* **2018**, 53, 135–140.

[89] Z. Liang, Y. Zhang, M. Souri, X. Luo, A. M. Boehm, R. Li, Y. Zhang, T. Wang, D.-Y. Kim, J. Mei, S. R. Marder and K. R. Graham, *J. Mater. Chem.A* **2018**, 6 (34), 16495–16505.

[90] S. Nam, J. Kim, H. Lee, H. Kim, C.-S. Ha and Y. Kim, *ACS Appl. Mater. Inter.* **2012**, 4 (3), 1281–1288.

[91] S. N. Patel, A. M. Glaudell, D. Kiefer and M. L. Chabinyc, *ACS Macro Lett.* **2016**, 5 (3), 268–272.

[92] Y. Cao, P. Smith and A. J. Heeger, *Synth. Met.* **1992**, 48 (1), 91–97.

[93] M. Chayer, K. Faïd and M. Leclerc, *Chem. Mater.* **1997**, 9 (12), 2902–2905.

[94] R. H. Karlsson, A. Herland, M. Hamedi, J. A. Wigenius, A. Åslund, X. Liu, M. Fahlman, O. Inganäs and P. Konradsson, *Chem. Mater.* **2009**, 21 (9), 1815–1821.

[95] A. I. Hofmann, R. Kroon, L. Yu and C. Müller, *J. Mater. Chem. C* **2018**, 6 (26), 6905–6910.

[96] R. J. Mammone and A. G. MacDiarmid, *J. Chem. Soc., Faraday Trans.* **1985**, 81 (1), 105.

[97] O. Bubnova, Z. U. Khan, H. Wang, S. Braun, D. R. Evans, M. Fabretto, P. Hojati-Talemi, D. Dagnelund, J.-B. Arlin, Y. H. Geerts, S. Desbief, D. W. Breiby, J. W. Andreasen, R. Lazzaroni, W. M. Chen, I. Zozoulenko, M. Fahlman, P. J. Murphy, M. Berggren and X. Crispin, *Nat. Mater.* **2013**, 13 (2), 190–194.

[98] Q. Wei, M. Mukaida, K. Kirihara, Y. Naitoh and T. Ishida, *Materials* **2015**, 8 (2), 732–750.

[99] D. Mantione, I. del Agua, A. Sanchez-Sanchez and D. Mecerreyes, *Polymers* **2017**, 9 (12), 354.

[100] P. Pingel, M. Arvind, L. Kölln, R. Steyrleuthner, F. Kraffert, J. Behrends, S. Janietz and D. Neher, *Adv. Electron. Mater.* **2016**, 2 (10), 1600204.

[101] Y. Han, G. Barnes, Y.-H. Lin, J. Martin, M. Al-Hashimi, S. Y. AlQaradawi, T. D. Anthopoulos and M. Heeney, *Chem. Mater.* **2016**, 28 (21), 8016–8024.

[102] M. Lu, H. T. Nicolai, G.-J. A. H. Wetzelaer and P. W. M. Blom, *Appl. Phys. Lett.* **2011**, 99 (17), 173302.

[103] R. A. Schlitz, F. G. Brunetti, A. M. Glaudell, P. L. Miller, M. A. Brady, C. J. Takacs, C. J. Hawker and M. L. Chabinyc, *Adv. Mater.* **2014**, 26 (18), 2825–2830.

[104] B. D. Naab, S. Zhang, K. Vandewal, A. Salleo, S. Barlow, S. R. Marder and Z. Bao, *Adv. Mater.* **2014**, 26 (25), 4268–4272.

[105] W. Ma, K. Shi, Y. Wu, Z.-Y. Lu, H.-Y. Liu, J.-Y. Wang and J. Pei, *ACS Appl. Mater. Inter.* **2016**, 8 (37), 24737–24743.

[106] K. Shi, F. Zhang, C.-A. Di, T.-W. Yan, Y. Zou, X. Zhou, D. Zhu, J.-Y. Wang and J. Pei, *J. Am. Chem. Soc.* **2015**, 137 (22), 6979–6982.

[107] S. Wang, H. Sun, U. Ail, M. Vagin, P. O. Å. Persson, J. W. Andreasen, W. Thiel, M. Berggren, X. Crispin, D. Fazzi and S. Fabiano, *Adv. Mater.* **2016**, 28 (48), 10764–10771.

[108] B. D. Naab, S. Guo, S. Olthof, E. G. B. Evans, P. Wei, G. L. Millhauser, A. Kahn, S. Barlow, S. R. Marder and Z. Bao, *J. Am. Chem. Soc.* **2013**, 135 (40), 15018–15025.

[109] S. Rossbauer, C. Müller and T. D. Anthopoulos, *Adv. Funct. Mater.* **2014**, 24 (45), 7116–7124.

[110] B. D. Naab, X. Gu, T. Kurosawa, J. W. F. To, A. Salleo and Z. Bao, *Adv. Electron. Mater.* **2016**, 2 (5), 1600004.

[111] D. Yuan, D. Huang, C. Zhang, Y. Zou, C. an Di, X. Zhu and D. Zhu, *ACS Appl. Mater. Inter.* **2017**, 9 (34), 28795–28801.

[112] S. Guo, S. K. Mohapatra, A. Romanov, T. V. Timofeeva, K. I. Hardcastle, K. Yesudas, C. Risko, J.-L. Brédas, S. R. Marder and S. Barlow, *Chem. Eur. J.* **2012**, 18 (46), 14760–14772.

[113] X. Lin, B. Wegner, K. M. Lee, M. A. Fusella, F. Zhang, K. Moudgil, B. P. Rand, S. Barlow, S. R. Marder, N. Koch and A. Kahn, *Nat. Mater.* **2017**, 16 (12), 1209–1215.

[114] C. Gaul, S. Hutsch, M. Schwarze, K. S. Schellhammer, F. Bussolotti, S. Kera, G. Cuniberti, K. Leo and F. Ortmann, *Nat. Mater.* **2018**, 17 (5), 439–444.

[115] E. E. Perry, C.-Y. Chiu, K. Moudgil, R. A. Schlitz, C. J. Takacs, K. A. O'Hara, J. G. Labram, A. M. Glaudell, J. B. Sherman, S. Barlow, C. J. Hawker, S. R. Marder and M. L. Chabinyc, *Chem. Mater.* **2017**, 29 (22), 9742–9750.

[116] O. Bubnova, Z. U. Khan, A. Malti, S. Braun, M. Fahlman, M. Berggren and X. Crispin, *Nat. Mater.* **2011**, 10 (6), 429–433.

[117] H. Klos, I. Rystau, W. Schütz, B. Gotschy, A. Skiebe and A. Hirsch, *Chem. Phys. Lett.* **1994**, 224 (3-4), 333–337.

[118] K. Mizoguchi, M. Machino, H. Sakamoto, M. Tokumoto, T. Kawamoto, A. Omerzu and D. Mihailovic, *Synth. Met.* **2001**, 121 (1-3), 1778–1779.

[119] S. Wang, H. Sun, T. Erdmann, G. Wang, D. Fazzi, U. Lappan, Y. Puttisong, Z. Chen, M. Berggren, X. Crispin, A. Kiriy, B. Voit, T. J. Marks, S. Fabiano and A. Facchetti, *Adv. Mater.* **2018**, 30 (31), 1801898.

[120] S. Fabiano, S. Braun, X. Liu, E. Weverberghs, P. Gerbaux, M. Fahlman, M. Berggren and X. Crispin, *Adv. Mater.* **2014**, 26 (34), 6000–6006.

[121] B. Sun, W. Hong, E. S. Thibau, H. Aziz, Z.-H. Lu and Y. Li, *ACS Appl. Mater. Inter.* **2015**, 7 (33), 18662–18671.

[122] J. Zhang, R. Xue, G. Xu, W. Chen, G.-Q. Bian, C. Wei, Y. Li and Y. Li, *Adv. Funct. Mater.* **2018**, 28 (13), 1705847.

[123] B. Russ, M. J. Robb, B. C. Popere, E. E. Perry, C.-K. Mai, S. L. Fronk, S. N. Patel, T. E. Mates, G. C. Bazan, J. J. Urban, M. L. Chabinyc, C. J. Hawker and R. A. Segalman, *Chem. Sci.* **2016**, 7 (3), 1914–1919.

[124] C. G. Tang, M. C. Y. Ang, K.-K. Choo, V. Keerthi, J.-K. Tan, M. N. Syafiqah, T. Kugler, J. H. Burroughes, R.-Q. Png, L.-L. Chua and P. K. H. Ho, *Nature* **2016**, 539 (7630), 536–540.

[125] W.-L. Seah, C. G. Tang, R.-Q. Png, V. Keerthi, C. Zhao, H. Guo, J.-G. Yang, M. Zhou, P. K. H. Ho and L.-L. Chua, *Adv. Funct. Mater.* **2017**, 27 (18), 1606291.

[126] C. D. Weber, C. Bradley and M. C. Lonergan, *J. Mater. Chem. A* **2014**, 2 (2), 303–307.

[127] D. T. Scholes, P. Y. Yee, J. R. Lindemuth, H. Kang, J. Onorato, R. Ghosh, C. K. Luscombe, F. C. Spano, S. H. Tolbert and B. J. Schwartz, *Adv. Funct. Mater.* **2017**, 27 (44), 1702654.

[128] R. Kroon, J. D. Ryan, D. Kiefer, L. Yu, J. Hynynen, E. Olsson and C. Müller, *Adv. Funct. Mater.* **2017**, 27 (47), 1704183.

[129] B. Lüssem, M. Riede and K. Leo, *Status Solidi A-Appl. Mat.* **2012**, 210 (1), 9–43.

[130] Y. Zhang, H. Zhou, J. Seifter, L. Ying, A. Mikhailovsky, A. J. Heeger, G. C. Bazan and T.-Q. Nguyen, *Adv. Mater.* **2013**, 25 (48), 7038–7044.

[131] Y. Li, J.-Y. Liu, Y.-D. Zhao and Y.-C. Cao, *Mater. Today* **2017**, 20 (5), 258–266.

[132] O. Bubnova and X. Crispin, *Energ. Environ. Sci.* **2012**, 5 (11), 9345.

[133] G.-H. Kim, L. Shao, K. Zhang and K. P. Pipe, *Nat. Mater.* **2013**, 12 (8), 719–723.

[134] S. H. Lee, H. Park, W. Son, H. H. Choi and J. H. Kim, *J. Mater. Chem. A* **2014**, 2 (33), 13380–13387.

[135] M. Culebras, C. M. Gómez and A. Cantarero, *J. Mater. Chem. A* **2014**, 2 (26), 10109–10115.

[136] E. Lim, K. A. Peterson, G. M. Su and M. L. Chabinyc, *Chem. Mater.* **2018**, 30 (3), 998–1010.

[137] H. Li, M. E. DeCoster, R. M. Ireland, J. Song, P. E. Hopkins and H. E. Katz, *J. Am. Chem. Soc.* **2017**, 139 (32), 11149–11157.

[138] R. Kroon, D. Kiefer, D. Stegerer, L. Yu, M. Sommer and C. Müller, *Adv. Mater.* **2017**, 29 (24), 1700930.

[139] J. Sun, M.-L. Yeh, B. J. Jung, B. Zhang, J. Feser, A. Majumdar and H. E. Katz, *Macromolecules* **2010**, 43 (6), 2897–2903.

[140] G. Zuo, X. Liu, M. Fahlman and M. Kemerink, *Adv. Funct. Mater.* **2017**, 28 (15), 1703280.

[141] G. Zuo, X. Liu, M. Fahlman and M. Kemerink, *ACS Appl. Mater. Inter.* **2018**, 10 (11), 9638–9644.

[142] D. de Leeuw, M. Simenon, A. Brown and R. Einerhand, *Synth. Met.* **1997**, 87 (1), 53–59.

[143] Y. Wang, M. Nakano, T. Michinobu, Y. Kiyota, T. Mori and K. Takimiya, *Macromolecules* **2017**, 50 (3), 857–864.

[144] D. Nava, Y. Shin, M. Massetti, X. Jiao, T. Biskup, M. S. Jagadeesh, A. Calloni, L. Duò, G. Lanzani, C. R. McNeill, M. Sommer and M. Caironi, *ACS Appl. Energy Mater.* **2018**, 1 (9), 4626–4634.

[145] Z. Q. Gao, B. X. Mi, G. Z. Xu, Y. Q. Wan, M. L. Gong, K. W. Cheah and C. H. Chen, *Chem. Commun.* **2008**, 0 (1), 117–119.

[146] D. Kiefer, A. Giovannitti, H. Sun, T. Biskup, A. Hofmann, M. Koopmans, C. Cendra, S. Weber, L. J. Anton Koster, E. Olsson, J. Rivnay, S. Fabiano, I. McCulloch and C. Müller, *ACS Energy Lett.* **2018**, 3 (2), 278–285.

[147] D. Abbaszadeh, A. Kunz, G. A. H. Wetzelaer, J. J. Michels, N. I. Crăciun, K. Koynov, I. Lieberwirth and P. W. M. Blom, *Nat. Mater.* **2016**, 15 (6), 628–633.

[148] S. Goffri, C. Müller, N. Stingelin-Stutzmann, D. W. Breiby, C. P. Radano, J. W. Andreasen, R. Thompson, R. A. J. Janssen, M. M. Nielsen, P. Smith and H. Sirringhaus, *Nat. Mater.* **2006**, 5 (12), 950–956.

[149] T. A. M. Ferenczi, C. Müller, D. D. C. Bradley, P. Smith, J. Nelson and N. Stingelin, *Adv. Mater.* **2011**, 23 (35), 4093–4097.

[150] Y. Huang, W. Wen, S. Mukherjee, H. Ade, E. J. Kramer and G. C. Bazan, *Adv. Mater.* **2014**, 26 (24), 4168–4172.

[151] V. Jousseaume, M. Morsli, A. Bonnet, O. Tesson and S. Lefrant, *J. Appl. Polym. Sci.* **1998**, 67 (7), 1205–1208.

[152] G. Lu, L. Bu, S. Li and X. Yang, *Adv. Mater.* **2014**, 26 (15), 2359–2364.

[153] G. Lu, H. Tang, Y. Huan, S. Li, L. Li, Y. Wang and X. Yang, *Adv. Funct. Mater.* **2010**, 20 (11), 1714–1720.

[154] A. J. Granero, P. Wagner, K. Wagner, J. M. Razal, G. G. Wallace and M. in het Panhuis, *Adv. Funct. Mater.* **2011**, 21 (5), 955–962.

[155] C. Hellmann, F. Paquin, N. D. Treat, A. Bruno, L. X. Reynolds, S. A. Haque, P. N. Stavrinou, C. Silva and N. Stingelin, *Adv. Mater.* **2013**, 25 (35), 4906–4911.

[156] C. Hellmann, N. D. Treat, A. D. Scaccabarozzi, J. R. Hollis, F. D. Fleischli, J. H. Bannock, J. de Mello, J. J. Michels, J.-S. Kim and N. Stingelin, *J. Polym. Sci., Part B: Polym. Phys.* **2014**, 53 (4), 304–310.

[157] G. W. Gokel, W. M. Leevy and M. E. Weber, *Chem. Rev.* **2004**, 104 (5), 2723–2750.

[158] Z. Xue, D. He and X. Xie, *J. Mater. Chem. A* **2015**, 3 (38), 19218–19253.

[159] Y. Matsushita, *Encyclopedia of Polymeric Nanomaterials*, Springer Berlin Heidelberg, **2014**, 1–6.

[160] H. Erothu, A. A. Sohdi, A. C. Kumar, A. J. Sutherland, C. Dagron-Lartigau, A. Allal, R. C. Hiorns and P. D. Topham, *Polym. Chem.* **2013**, 4 (13), 3652.

[161] M. J. Dyson, E. Lariou, J. Martin, R. Li, H. Erothu, G. Wantz, P. D. Topham, O. J. Dautel, S. C. Hayes, P. N. Stavrinou and N. Stingelin, *Chem. Mater.* **2019**, DOI: 10.1021/acs.chemmater.8b05259.

[162] C. C. Chen and J. L. White, *Polym. Eng. Sci.* **1993**, 33 (14), 923–930.

[163] J. Mei and Z. Bao, *Chem. Mater.* **2013**, 26 (1), 604–615.

[164] A. Giovannitti, D.-T. Sbircea, S. Inal, C. B. Nielsen, E. Bandiello, D. A. Hanifi, M. Sessolo, G. G. Malliaras, I. McCulloch and J. Rivnay, *Proc. Natl. Acad. Sci. U.S.A.* **2016**, 113 (43), 12017–12022.

[165] C. B. Nielsen, A. Giovannitti, D.-T. Sbircea, E. Bandiello, M. R. Niazi, D. A. Hanifi, M. Sessolo, A. Amassian, G. G. Malliaras, J. Rivnay and I. McCulloch, *J. Am. Chem. Soc.* **2016**, 138 (32), 10252–10259.

[166] A. Giovannitti, C. B. Nielsen, D.-T. Sbircea, S. Inal, M. Donahue, M. R. Niazi, D. A. Hanifi, A. Amassian, G. G. Malliaras, J. Rivnay and I. McCulloch, *Nat. Commun.* **2016**, 7 (1), 13066.

[167] C. K. Song, B. J. Eckstein, T. L. D. Tam, L. Trahey and T. J. Marks, *ACS Appl. Mater. Inter.* **2014**, 6 (21), 19347–19354.

[168] D. Moia, A. Giovannitti, A. A. Szumska, I. P. Maria, E. Rezasoltani, M. Sachs, M. Schnurr, P. R. F. Barnes, I. McCulloch and J. Nelson, *Energ. Environ. Sci.* **2019**, 12 (4), 1349–1357.

[169] D. T. McQuade, A. E. Pullen and T. M. Swager, *Chem. Rev.* **2000**, 100 (7), 2537–2574.

[170] J. Brebels, J. V. Manca, L. Lutsen, D. Vanderzande and W. Maes, *J. Mater. Chem.A* **2017**, 5 (46), 24037–24050.

[171] J. Li, C. W. Rochester, I. E. Jacobs, E. W. Aasen, S. Friedrich, P. Stroeve and A. J. Moulé, *Org. Electron.* **2016**, 33, 23–31.

[172] P. Wei, J. H. Oh, G. Dong and Z. Bao, *J. Am. Chem. Soc.* **2010**, 132 (26), 8852–8853.

[173] J. Liu, L. Qiu, R. Alessandri, X. Qiu, G. Portale, J. Dong, W. Talsma, G. Ye, A. A. Sengrian, P. C. T. Souza, M. A. Loi, R. C. Chiechi, S. J. Marrink, J. C. Hummelen and L. J. A. Koster, *Adv. Mater.* **2018**, 30 (7), 1704630.

[174] H. Yan, Z. Chen, Y. Zheng, C. Newman, J. R. Quinn, F. Dötz, M. Kastler and A. Facchetti, *Nature* **2009**, 457 (7230), 679–686.

[175] J. Liu, L. Qiu, G. Portale, M. Koopmans, G. ten Brink, J. C. Hummelen and L. J. A. Koster, *Adv. Mater.* **2017**, 29 (36), 1701641.

[176] J. Liu, L. Qiu, G. Portale, S. Torabi, M. C. A. Stuart, X. Qiu, M. Koopmans, R. C. Chiechi, J. C. Hummelen and L. J. A. Koster, *Nano Energy* **2018**, 52, 183–191.

[177] Z. Yi, S. Wang and Y. Liu, *Adv. Mater.* **2015**, 27 (24), 3589–3606.

[178] P. K. Koech, A. B. Padmaperuma, L. Wang, J. S. Swensen, E. Polikarpov, J. T. Darsell, J. E. Rainbolt and D. J. Gaspar, *Chem. Mater.* **2010**, 22 (13), 3926–3932.

[179] J. E. Rainbolt, P. K. Koech, E. Polikarpov, J. S. Swensen, L. Cosimbescu, A. V. Ruden, L. Wang, L. S. Sapochak, A. B. Padmaperuma and D. J. Gaspar, *J. Mater. Chem. C* **2013**, 1 (9), 1876.

[180] X.-Q. Zhu, M.-T. Zhang, A. Yu, C.-H. Wang and J.-P. Cheng, *J. Am. Chem. Soc.* **2008**, 130 (8), 2501–2516.

[181] L. Qiu, J. Liu, R. Alessandri, X. Qiu, M. Koopmans, R. W. A. Havenith, S. J. Marrink, R. C. Chiechi, L. J. A. Koster and J. C. Hummelen, *J. Mater. Chem. A* **2017**, 5 (40), 21234–21241.

[182] J. Li, C. Koshnick, S. O. Diallo, S. Ackling, D. M. Huang, I. E. Jacobs, T. F. Harrelson, K. Hong, G. Zhang, J. Beckett, M. Mascal and A. J. Moulé, *Macromolecules* **2017**, 50 (14), 5476–5489.

[183] M. L. Tietze, J. Benduhn, P. Pahner, B. Nell, M. Schwarze, H. Kleemann, M. Krammer, K. Zojer, K. Vandewal and K. Leo, *Nat. Commun.* **2018**, 9 (1), 1182.

[184] A. Mityashin, Y. Olivier, T. V. Regemorter, C. Rolin, S. Verlaak, N. G. Martinelli, D. Beljonne, J. Cornil, J. Genoe and P. Heremans, *Adv. Mater.* **2012**, 24 (12), 1535–1539.

[185] J. B. Torrance, J. E. Vazquez, J. J. Mayerle and V. Y. Lee, *Phys. Rev. Lett.* **1981**, 46 (4), 253–257.

[186] J. Saska, G. Gonel, Z. I. Bedolla-Valdez, S. D. Aronow, N. E. Shevchenko, A. S. Dudnik, A. J. Moulé and M. Mascal, *Chem. Mater.* **2019**, 31 (5), 1500–1506.

[187] D. Walker and J. D. Hiebert, *Chem. Rev.* **1967**, 67 (2), 153–195.

[188] DDQ is well known for its use as oxidative reaction agent in organic synthesis and can be bought in large scale at a low price. The average price per gram for DDQ available from Sigma-Aldrich/Merck was about 400 times lower than for F4TCNQ at the time this thesis was written.

[189] P. Panda, D. Veldman, J. Sweelssen, J. J. A. M. Bastiaansen, B. M. W. Langeveld-Voss and S. C. J. Meskers, *J. Phys. Chem. B* **2007**, 111 (19), 5076–5081.

[190] L. Tolbert, C. Edmond and J. Kowalik, *Synth. Met.* **1999**, 101 (1-3), 500–501.

[191] M. Maitrot, G. Guillaud, B. Boudjema, J. J. André and J. Simon, *J. Appl. Phys.* **1986**, 60 (7), 2396–2400.

[192] A. K. Thomas, R. Johnson, B. W. Stein, M. L. Kirk, H. Guo and J. K. Grey, *J. Phys. Chem. C* **2017**, 121 (42), 23817–23826.

[193] B. Neelamraju, K. E. Watts, J. E. Pemberton and E. L. Ratcliff, *J. Phys. Chem. Lett.* **2018**, 9 (23), 6871–6877.

[194] M. Pfeiffer, T. Fritz, J. Blochwitz, A. Nollau, B. Plönnigs, A. Beyer and K. Leo, *Adv. Solid State Phys.* **1999**, 39, 77–90.

[195] V. I. Arkhipov, E. V. Emelianova, P. Heremans and H. Bässler, *Phys. Rev. B* **2005**, 72 (23), 235202.

[196] V. I. Arkhipov, P. Heremans, E. V. Emelianova and H. Bässler, *Phys. Rev. B* **2005**, 71 (4), 045214.

[197] J. Lu, T. H. Le, D. A. K. Traore, M. Wilce, A. M. Bond and L. L. Martin, *J. Org. Chem.* **2012**, 77 (23), 10568–10574.

[198] A. L. Sutton, B. F. Abrahams, D. M. D'Alessandro, R. W. Elliott, T. A. Hudson, R. Robson and P. M. Usov, *CrystEngComm* **2014**, 16 (24), 5234.

[199] D. A. Dixon, J. C. Calabrese and J. S. Miller, *J. Phys. Chem.* **1989**, 93 (6), 2284–2291.

[200] S. Panja, U. Kadhane, J. U. Andersen, A. I. S. Holm, P. Hvelplund, M.-B. S. Kirketerp, S. B. Nielsen, K. Støchkel, R. N. Compton, J. S. Forster, K. Kilså and M. B. Nielsen, *J. Chem. Phys.* **2007**, 127 (12), 124301.

[201] L. Ma, P. Hu, H. Jiang, C. Kloc, H. Sun, C. Soci, A. A. Voityuk, M. E. Michel-Beyerle and G. G. Gurzadyan, *Sci. Rep.* **2016**, 6 (1), 28510.

[202] K. Do, D. M. Huang, R. Faller and A. J. Moulé, *Phys. Chem. Chem. Phys.* **2010**, 12 (44), 14735.

[203] Y. Karpov, T. Erdmann, M. Stamm, U. Lappan, O. Guskova, M. Malanin, I. Raguzin, T. Beryozkina, V. Bakulev, F. Günther, S. Gemming, G. Seifert, M. Hambsch, S. Mannsfeld, B. Voit and A. Kiriy, *Macromolecules* **2017**, 50 (3), 914–926.

[204] J. Nelson, *Mater. Today* **2011**, 14 (10), 462–470.

[205] P. Yang, M. Yuan, D. F. Zeigler, S. E. Watkins, J. A. Lee and C. K. Luscombe, *J. Mater. Chem. C* **2014**, 2 (17), 3278–3284.

[206] M. Lenes, F. B. Kooistra, J. C. Hummelen, I. V. Severen, L. Lutsen, D. Vanderzande, T. J. Cleij and P. W. M. Blom, *J. Appl. Phys.* **2008**, 104 (11), 114517.

[207] I. Constantinou, X. Yi, N. T. Shewmon, E. D. Klump, C. Peng, S. Garakyaraghi, C. K. Lo, J. R. Reynolds, F. N. Castellano and F. So, *Adv. Energy Mater.* **2017**, 7 (13), 1601947.

[208] J. Liu, S. Maity, N. Roosloot, X. Qiu, L. Qiu, R. C. Chiechi, J. C. Hummelen, E. von Hauff and L. J. A. Koster, *Adv. Electron. Mater.* **2019**, 1800959.

[209] R. Ghosh, A. R. Chew, J. Onorato, V. Pakhnyuk, C. K. Luscombe, A. Salleo and F. C. Spano, *J. Phys. Chem. C* **2018**, 122 (31), 18048–18060.

[210] T. J. Aubry, J. C. Axtell, V. M. Basile, K. J. Winchell, J. R. Lindemuth, T. M. Porter, J.-Y. Liu, A. N. Alexandrova, C. P. Kubiak, S. H. Tolbert, A. M. Spokoyny and B. J. Schwartz, *Adv. Mater.* **2019**, 31 (11), 1805647.

[211] L. Müller, D. Nanova, T. Glaser, S. Beck, A. Pucci, A. K. Kast, R. R. Schröder, E. Mankel, P. Pingel, D. Neher, W. Kowalsky and R. Lovrincic, *Chem. Mater.* **2016**, 28 (12), 4432–4439.

[212] E. Hückel, *Ergebnisse der Exakten Naturwissenschaften*, Springer Berlin Heidelberg, **1924**, 199–276.

[213] J.-L. Burgot, *The Notion of Activity in Chemistry*, Springer International Publishing, **2017**.

[214] D. H. Evans, *Chem. Rev.* **2008**, 108 (7), 2113–2144.

[215] E. K. Lee, M. Y. Lee, C. H. Park, H. R. Lee and J. H. Oh, *Adv. Mater.* **2017**, 29 (44), 1703638.

[216] O. V. Kozlov and S. A. Zapunidi, *Synth. Met.* **2013**, 169, 48–54.

[217] P. Tyagi, M. K. Dalai, C. K. Suman, S. Tuli and R. Srivastava, *RSC Adv.* **2013**, 3 (46), 24553.

[218] J. Li, C. W. Rochester, I. E. Jacobs, S. Friedrich, P. Stroeve, M. Riede and A. J. Moulé, *ACS Appl. Mater. Inter.* **2015**, 7 (51), 28420–28428.

[219] L. Müller, S.-Y. Rhim, V. Sivanesan, D. Wang, S. Hietzschold, P. Reiser, E. Mankel, S. Beck, S. Barlow, S. R. Marder, A. Pucci, W. Kowalsky and R. Lovrincic, *Adv. Mater.* **2017**, 29 (30), 1701466.

[220] H. Hase, K. O'Neill, J. Frisch, A. Opitz, N. Koch and I. Salzmann, *J. Phys. Chem. C* **2018**, 122 (45), 25893–25899.

[221] M. R. Andersson, O. Thomas, W. Mammo, M. Svensson, M. Theander and O. Inganäs, *J. Mater. Chem.* **1999**, 9 (9), 1933–1940.

[222] C. Wang, D. T. Duong, K. Vandewal, J. Rivnay and A. Salleo, *Phys. Rev. B* **2015**, 91 (8), 085205.

[223] R. Di Pietro, D. Fazzi, T. B. Kehoe and H. Sirringhaus, *J. Am. Chem. Soc.* **2012**, 134 (36), 14877–14889.

[224] M. L. Tietze, B. D. Rose, M. Schwarze, A. Fischer, S. Runge, J. Blochwitz-Nimoth, B. Lüssem, K. Leo and J.-L. Brédas, *Adv. Funct. Mater.* **2016**, 26 (21), 3730–3737.

[225] B. A. Jones, M. J. Ahrens, M.-H. Yoon, A. Facchetti, T. J. Marks and M. R. Wasielewski, *Angew. Chem. Int. Ed.* **2004**, 43 (46), 6363–6366.

[226] B. A. Jones, A. Facchetti, M. R. Wasielewski and T. J. Marks, *J. Am. Chem. Soc.* **2007**, 129 (49), 15259–15278.

[227] X. Gao, C. an Di, Y. Hu, X. Yang, H. Fan, F. Zhang, Y. Liu, H. Li and D. Zhu, *J. Am. Chem. Soc.* **2010**, 132 (11), 3697–3699.

[228] J. Li, J.-J. Chang, H. S. Tan, H. Jiang, X. Chen, Z. Chen, J. Zhang and J. Wu, *Chem. Sci.* **2012**, 3 (3), 846–850.

[229] G.-S. Ryu, Z. Chen, H. Usta, Y.-Y. Noh and A. Facchetti, *MRS Commun.* **2016**, 6 (01), 47–60.

[230] Y. hun Shin, A. Welford, H. Komber, R. Matsidik, T. Thurn-Albrecht, C. R. McNeill and M. Sommer, *Macromolecules* **2018**, 51 (3), 984–991.

[231] A. Savva, C. Cendra, A. Giugni, B. Torre, J. Surgailis, D. Ohayon, A. Giovannitti, I. McCulloch, E. D. Fabrizio, A. Salleo, J. Rivnay and S. Inal, *Chem. Mater.* **2019**, 31 (3), 927–937.